RESPONSE OF A PLASTIC CIRCULAR PLATE TO A DISTRIBUTED TIME-VARYING LOADING

By

Deene J. Weidman

Thesis submitted to the Graduate Faculty of the

Virginia Polytechnic Institute

in candidacy for the degree of

DOCTOR OF PHILOSOPHY

in

Engineering Mechanics

June 1968

RESPONSE OF A PLASTIC CIRCULAR PLATE TO A DISTRIBUTED TIME-VARYING LOADING

by

Deene J. Weidman

Thesis submitted to the Graduate Faculty of the

Virginia Polytechnic Institute

in partial fulfillment for the degree of

DOCTOR OF PHILOSOPHY

in

Engineering Mechanics

APPROVED:

Chairman, Prof. F. J. Maher

Prof. R. L. Armstrong

Prof. V. G. Maderspach

Prof. W. E. Pace

Prof. J. Counts

June 1968

Blacksburg, Virginia

KLB 5-30-74

TABLE OF CONTENTS

ACKNOWLEDGMENTS

The author wishes to express his appreciation to several persons without whose help this dissertation would not have been written. The author explicitly wishes to thank Prof. F. Maher of the Engineering Mechanics Department at Virginia Polytechnic Institute for his assistance at every possible opportunity and his firm encouragement to complete the work. Also, the author must thank Prof. R. Armstrong of the Engineering Mechanics Department at Virginia Polytechnic Institute for his very helpful suggestions and comments that broadened the author's insights and actually allowed the full problem to be attempted. Finally, the author must acknowledge the assistance of his secretary,

, during the difficult typing of the manuscript, as well as thank his wife and family for their understanding.

INTRODUCTION

The prediction of the plastic response of a simply supported circular plate has been a problem of considerable interest in recent years. Much of the current knowledge in plastic-plate problems stems from original analyses instituted at Brown University in the early 1950's by H. G. Hopkins and W. Prager and others. In these early papers, the plastic-plate material was considered to follow the Tresca yield criterion and the loading was considered to be uniform over an annular or circular region on the surface of the plate and statically applied. The load-carrying capacity (or load at which the initial yielding occurs) was determined and the rate of deflection was found. Even though these earlier papers (as examples, see refs. 1 through 6) solved for only a few of the quantities of interest in plastic-plate theory, these papers presented a basic approach to the analysis of general plasticity problems.

After the first few papers on plastic plates were published and the significance of these analyses was realized, many more extensive analyses were initiated and other effects were investigated. The influence of changing the yield condition from the Tresca yield condition to other forms (von Mises, etc.) was investigated (refs. 4 and 7) and relatively small differences in carrying capacity were noted due to the change of yield condition (for the various loadings considered).

The influence of including the inplane forces and thus allowing for membrane action, has also been investigated (refs. 8 through 14) and this effect is shown to cause the deflection to be reduced from the deflection due to bending theory. This is a very difficult problem

involving the interaction of several yield variables (two bending moments and two inplane forces). Sometimes the interactions between moments and forces are neglected (see refs. 13 and 14 for current interaction theories). These inplane forces are present in plastic-plate problems as soon as deflection starts, and become increasingly important as deflections increase. Initially, bending action strongly predominates, indicating that membrane forces start to have a significant effect only when the plate central deflection becomes greater than about twice the plate thickness. Thus, if the initiation of deflection is of primary interest, then the need for inclusion of membrane forces is greatly reduced. These membrane analyses (refs. 8-14) included small computational approximations in addition to the assumption of a uniformly distributed impulsive loading. Thus, a bending and membrane solution for a plate under a loading that varies with radius and time is still not available, and the results presented for uniformly distributed impulsive loadings may not be directly applicable to more general loading cases.

The consideration of additional material properties such as strain hardening, viscosity, elastic deformation etc., has also been made (refs. 7, 9, and 15 through 17). In these references, consideration of any one of these properties allowed the theoretical analysis to predict the experimental results well. For example, reference 7 shows that the addition of viscosity effects could yield agreement of the theoretical with experimental final maximum deflections; however, the magnitude of the viscosity coefficient is unknown, and its value was selected for the specific case of a uniformly distributed impulsive loading.

Interaction problems have also been receiving attention more recently (see refs. 18 through 21). Interaction problems are defined as those problems in which more than two stress resultants are considered necessary to define the yield surface. The analyses including inplane forces (refs. 8 through 14) are examples of this type of problem. A three- or four-dimensional yield surface is needed, with each stress resultant allowed a range of values before it causes yielding by itself. Within this range of values, an interaction exists between all of the allowed stress resultants. Most often, the interaction is determined to be either linear or quadratic in these stress resultants. The influence of shear forces (see ref. 21) is a particularly important interaction problem that has not been widely analyzed. For example, even though it is a well-recognized fact that shear forces are of primary importance for concentrated load problems, bending theory has still been used to predict the loading-carrying capacity of plates under a concentrated load. Also, the success of using a viscous-shearing model of failure for ballistic impact problems (ref. 22) indicates the need for the consideration of shearing forces.

The investigation of other boundary conditions (such as clamped supports or elastic supports, refs. 23 through 25) and other geometries (such as annular plates, refs. 26 and 27) has also been initiated. An attempt to discuss all of the literature on the plastic theory of thin plates would not be appropriate here. An excellent group of bibliographies and reviews can be found in references 28 through 32. Those papers directly discussed and referenced herein are thought to be representative of the best of current work in this field.

Two experimental papers must be mentioned here as essential to proper justification of the theoretical analyses. Analyses employing piecewise linear yield surfaces indicate that points (or circles) should exist across which a discontinuity is expected. These discontinuities would not be expected for smooth yield surfaces. Such a discontinuity has been observed and recorded for a beam (ref. 33), yielding the definition of a hinge. More significantly, such a "hinge circle" has also been recorded for a thin plate (ref. 34). These experimental observations lend creditability to the use of piecewise linear yield surfaces, which have only been considered approximations in the past.

In nearly all of the papers referred to above, the radial variation of the loading was considered to be either uniform over all or part of the plate surface or concentrated at the plate center. The analysis of a more general radial load distribution is needed, and this variation is allowed in this thesis.

The solutions of the references centered around determining that unique single location in these plates at which the hinge circle occurs. Initially, static loadings were considered, but in a classic paper by Hopkins and Prager (ref. 2) the influence of a time variation was first considered. In this reference, a uniform load was applied over the surface of the plate for a finite length of time and then removed. This analysis introduced the fact that the location of the hinge circle does not remain fixed, but after the loading is removed, the hinge circle shrinks to a single point at the center of the plate. This moving

boundary separates two different regimes (or regions of solution) and causes many complications. The difficulty of the moving hinge circle is also important in impulsive loading problems, and therefore the problem of defining its motion had to be solved.

After the initial papers were presented, the investigation of impulsive loadings soon proceeded to dominate the literature (see, for example, refs. 5, 6, 8, 11, 18, 27, 35, and 36). A general radial variation of the loading on the plate has been attempted in only one case (ref. 36) where a Gaussian radial load distribution was assumed to be impulsively applied.

The solution of the response of a plastic plate to a general time variation of loading is a considerably more involved problem. The location of the hinge circle varies strongly if the loading changes with time. Very few references are available that allow time variation of loading (for example, refs. 2, 37, and 38). Considering only uniformly loaded plates, with a time variation that quickly decays toward zero and never increases, Perzyna (ref. 37) states that the actual shape of the time variation has very little effect on the final deflections. However, in this reference the uniform load is maintained on the plate for a considerable length of time before rapid removal of the load, and thus it might be expected to show only small variations due to load removal.

Sankaranarayanan (ref. 38), on the other hand, has shown that for spherical caps under a similar uniform loading the time variation of the loading greatly influenced the final deformation. Therefore,

a need is seen for the general determination of the motion of the hinge circle, and, indeed, this unique movement of the hinge circle is the key to solution of involved dynamic plasticity problems in plates.

Although this dissertation is concerned with the dynamic loading of simply supported, rigid-plastic plates, the basic problem that prompted the analysis is the ballistic impact problem. This problem is concerned with determination of the response of a plate when impacted by a projectile (or spray of projectiles) traveling at a high velocity. Retaining the integrity of the plate is of prime concern. At low impact velocities, the response of the plate is entirely elastic. As the projectile velocity increases, the response of the plate becomes predominantly plastic, and it is this problem of plasticity that is of interest herein. An excellent review of this impact problem (from the elastic point of view) is found in reference 39. The basic point of interest is that the loading on the plate is definitely not impulsive, or indeed, not even uniformly distributed across the surface of the impacted plate. Therefore, a general analysis allowing a loading variation in both radius and time is desired.

LIST OF SYMBOLS

a,α	parameters in example loading cases
b	outer radius of plate
C,C_i	arbitrary functions and constants used for solutions
$f(\sigma_i)$	functional form of the yield surface
$f_1(r,\rho,t)$	function used in solution for regime AB, see equation (50)
h	half-thickness of plate
$I_1(\rho,r),I_2(\rho,r)$	general functions defined by equations (57) and (58)
M	bending-moment resultant
M_o	yield-moment resultant, $\sigma_o h^2$
$p(t)$	time variation of applied loading
p_o	the value of loading at which initial hinge forms
p_1	the value of loading at which hinge occurs away from origin
p_{max}	maximum value of loading applied (maximum value of $p(t)$)
P_i	specific points on a general yield surface
$q(r)$	radial variation of applied loading
Q	shear force resultant
r,θ,z	radial, circumferential, and transverse coordinates, respectively
$R(r),T(t)$	functions for separation of variables solution, see equation (41)

s	coordinate along $\rho(t)$ curve, see figure 5
t	time
t_o	initial time
t_1	time hinge circle disappears
t^*	time plate comes to rest
$t(r)$	time needed for hinge to reach point r
$t(\rho)$	time needed for hinge to reach current location ρ
u	radial displacement in plate
V_o	arbitrary applied velocity for impulsive loading
w	plate deflection
β	general flow rule constant, see equation (33)
$\epsilon, \dot{\epsilon}$	strain and strain rate in plate, respectively
η, ξ	dummy variables of integration
$\dot{\kappa}$	curvature rate
μ	mass per unit area of plate
$\rho(t)$	general hinge circle location
ρ_o	initial hinge circle location
ρ_1, ρ_2	two general functions of ρ, see equation (65)
σ	an average stress, defined by equation (8)
σ_o	yield stress in simple tension or compression
σ_i	principal stress components
σ_z, τ_{rz}	vertical and shearing stresses, assumed small
τ_o	octahedral shear stress
$\tau_{r\theta}, \tau_{\theta z}$	shearing stresses

Subscripts

1,2	refer to two planar coordinates (often r and θ)
r,θ	refer to radial and circumferential quantities, respectively

Extra Symbols

$[\,]$	denotes the jump in a quantity across the hinge
$\vert$	denotes quantity evaluated at a given point

GENERAL PLASTICITY CONSIDERATIONS

In this section some of the basic considerations for any flow (or incremental) theory of plasticity are discussed. Several possible choices are evaluated, and from these choices the methods and cases considered in the body of the text are selected. These methods have been chosen to yield a theoretical solution to a general group of plasticity problems. This is done without recourse to a large digital computer program solving high-order, coupled differential equations and utilizing multivariable difference techniques, iteration procedures, etc., for a solution.

Yield Criteria and Flow Rules

Initially, a basic criterion of material yielding must be selected. The engineering material to be used, and the application to which it will ultimately be put, dictate the type of material yielding to consider. This philosophy of yielding (whether maximum tensile stress, maximum shear stress, etc.) defines the actual shape of the yield surface. Once the shape of the yield surface is determined, the generalized flow rule is applied. It is assumed herein that the material is always isotropic during flow, so that principal stress directions are the same as the principal strain-rate directions. The flow rule then states that the principal strain rates are in the same proportions as the direction cosines of the outward facing normal to the yield surface at that point. This approach breaks down only in cases where the yield surface has sharp corners, and the outward normal direction is not unique. Such cases are

important, since many yield surfaces do possess corners. However, additional information is available in such cases that allows a unique solution to be found. This fact will be illustrated later in this section.

In the case of an isotropic, perfectly plastic solid, the yield condition $f(\sigma_i) = 0$ can be considered as a three-dimensional surface in the principal stress space as shown in figure 1. The type of yield criterion selected would affect the yield condition $f(\sigma_i)$ and thus change the shape of this surface. The flow rule states that a relationship exists between a given point (σ_i) on the yield surface and the principal strain rates $(\dot{\epsilon}_i)$ at that point. The flow vector at a point on the yield surface has direction cosines with the ratios of $\dot{\epsilon}_i$ values, and is normal to $f(\sigma_i) = 0$, or

$$\dot{\epsilon}_j = \frac{\lambda \partial f(\sigma_i)}{\partial \sigma_j} \tag{1}$$

where the quantity λ is the constant of proportionality.

The flow rule is then a function of the local normal to the yield surface and at any point on the yield surface at which the normal is unique (say points P_1 and P_2 in fig. 1) the strain rate directions are well defined. Using strain displacement relationships or (taking time derivatives of these expressions) strain rate displacement rate expressions, the strain rates can be used to solve for the deflections in regions where the flow rule vector is well defined. However, at any point where the normal is not unique (say the point P_3 in fig. 1), the flow rule vector may lie anywhere within the cone of vectors that is

formed by the normals to all possible surfaces of $f(\sigma_i) = 0$ that pass through the given point. For the point P_3, it appears that one flow mechanism corresponds to the surface containing P_1, and another flow mechanism corresponds to the surface containing P_2, so that at the point P_3, a linear combination of these two mechanisms might be expected to occur. Thus, β times one flow mechanism is added to $(1 - \beta)$ times the other flow mechanism, to yield the combined mechanism at the point P_3. The constant, β, should then lie between 0 and 1. Note that the discontinuity between the P_1 and P_2 types of flow mechanisms disappears toward the rearward portion of the yield surface, indicating that, in general cases, the occurrence of sharp corners may vary with the state of stress (or even with time).

A short comment must be made concerning the influence of boundary conditions in yield criterion (or yield curve) selection. If a plane stress problem for a circular plate is assumed, the yield surface becomes a curve in the σ_1, σ_2 plane. A portion of this plane is shown in figure 2. The three points (marked +) must be on the yield surface, and if a simply-supported plate is being analyzed, only the shaded region A is to be considered ($\sigma_r = \sigma_\theta$ at the center of the plate, and $\sigma_r = 0$ at the outer edge). Any yield condition that has simple differential equations in this region is then of interest for simply-supported plates. However, if a clamped plate is being analyzed, both of the shaded regions A and B are of interest. An entirely different yield condition may have simpler differential equations in this larger region.

In summary, the procedure to follow is to first select a yielding criterion and from this criterion determine the yield surface. Next the

specific associated flow rules are written for that particular surface, and the necessary equations for solution are written. In all cases, care must be taken to include the desired material properties, and even to consider the boundary conditions of a specific problem when selecting the yield criterion. Current yield criteria are discussed in the following sections to illustrate the manner in which this approach is applied. In these sections it is assumed for simplicity of discussion that the plate under analysis is in a state of plane stress ($\sigma_3 = 0$), and the yield surfaces are drawn as curves in the (σ_1,σ_2) plane. It is important to note that, while the yield surface is considered a curve in the $\sigma_3 = 0$ plane, the normals to the three-dimensional surface are not in this (σ_1,σ_2) plane. However, the projection of these normal components onto the (σ_1,σ_2) plane is normal to the yield curve, and the principle of the flow vector is still applicable. Only bending stresses are considered herein, so that σ_1 and M_1 are related, as well as σ_2 and M_2. Thus, equations can be written in terms of either moments or stresses. Also it is a general fact that for an isotropic plastic body the yield surface is symmetric with respect to a 45° line through the origin. With these general thoughts in mind, the specific yield curves will now be discussed, considering the x_i coordinates are r, θ, and z, respectively.

Maximum octahedral shear stress - von Mises.- The octahedral shear stress is written in general as

$$\tau_o = \frac{1}{3}\sqrt{(\sigma_1 - \sigma_2)^2 + (\sigma_1 - \sigma_3)^2 + (\sigma_2 - \sigma_3)^2}$$

and, for the plane stress case of a circular plate of thickness $2h$

$$\sigma_1 = \sigma_r = \frac{M_r}{h^2} \qquad \sigma_2 = \sigma_\theta = \frac{M_\theta}{h^2} \qquad \sigma_3 = 0$$

and therefore

$$\sigma_o = \left(\frac{3}{\sqrt{2}}\right)\tau_o = \left(\frac{1}{\sqrt{2}}\right)\sqrt{(\sigma_r - \sigma_\theta)^2 + \sigma_r^2 + \sigma_\theta^2} \tag{2}$$

where σ_o is the yield stress in simple tension, and is related to the yield moment $\sigma_o = \frac{M_o}{h^2}$. In terms of the moment resultants, equation (2) can be written in the form of a yield surface equation as

$$M_r^2 + M_\theta^2 - M_r M_\theta - M_o^2 = 0 \tag{3}$$

If equation (3) is plotted in the M_r, M_θ plane, an ellipse (with its major axis at 45^o) is found as shown in figure 3.

In the equilibrium equations developed later, the differential equation for M_r contains a single term in M_θ, and this term is removed by solving equation (3) for M_θ and substituting into the equilibrium equation. From equation (3), then

$$M_\theta = \frac{M_r}{2} \pm \sqrt{M_o^2 - \frac{3}{4} M_r^2} \tag{4}$$

The upper sign refers to the upper half (above the major axis) of the yield surface and the lower sign to the lower half. From equation (4) it is seen that the expression for M_θ would cause a strongly nonlinear differential equation for M_r with a nonremovable square-root term.

Therefore, any approach utilizing the von Mises yield condition would usually require a large-size computer program for solution of all the variables involved. However, it may be noted that this yield surface is the only yield surface considered herein that is smooth and regular (no corners), and various plasticity regimes (particular regions of solution) need not be defined for such a yield function.

Maximum tensile stress - Johansen.- In the case of piecewise linear yield surfaces, the definition of the yield surface (or yield function) is not a continuous function as it was for the von Mises yield surface. Instead, piecewise linearity means that the statement of the conditions for yielding should be expressed as a maximum or set of maximum statements. For a homogeneous material with a low yield strength in tension (such as a uniformly mixed concrete, for example), the tensile stress governs the yielding of the material, and the yield condition can be written in the form

$$\max. \left\{ \left| \sigma_i \right| \right\} - \sigma_o = 0 \tag{5}$$

For the plane stress conditions considered herein, only the stresses σ_r and σ_θ are included. Then, if $|\sigma_r|$ is greater than $|\sigma_\theta|$, then $|\sigma_r| = |\sigma_o|$ is the yield condition. This portion of the yield surface consists of two straight vertical lines at $\sigma_r = \pm\sigma_o$, and $M_r = \pm M_o$ on these lines. The differential equation for M_r then just defines exactly M_θ, and the solution is completed. Similarly, for $|\sigma_\theta|$ greater than $|\sigma_r|$, the yield surface becomes two straight horizontal lines at $\sigma_\theta = \pm\sigma_o$ and $M_\theta = \pm M_o$ along these lines. The differential

equation for M_r is then solved exactly and the solution is again completed. The yield condition is therefore a square, and is shown in figure 4. The use of this yield criterion leads to simple, solvable differential equations to determine the moments and deflections. However, most metals have high tensile strengths and often fail in a shearing manner. Since the equations for the Johansen yield condition are quite similar in form to the equations for the Tresca yield condition (which is a shearing failure criterion) consideration of the Johansen yield surface is deferred here for future study.

Maximum shearing stress - Tresca.- The maximum shearing stress yield criterion of Tresca is by far the most often used yield criterion. It defines a piecewise linear yield surface, and, therefore, the equation of the surface is expressed as a maximum type of statement. All points on the yield surface have a maximum shear stress equal to $\frac{\sigma_o}{2}$, so that the equation of the yield surface (a six-sided surface in general) can be written

$$\max. \left\{ \frac{|\sigma_i - \sigma_j|}{2} \right\} - \frac{\sigma_o}{2} = 0 \qquad j \neq i \qquad (6)$$

Consideration of the plane stress problem analyzed herein ($\sigma_3 = 0$), and the yield condition of equation (6), the yield surface (in the σ_1, σ_2 plane) becomes a hexagon as shown in figure 4. Since $\sigma_3 = \sigma_z = 0$, the equations of the yield curve are directly written in terms of the moments as

$$h^2\sigma_\theta = M_\theta = \pm M_o \qquad h^2\sigma_r = M_r = \mp M_o \qquad M_r - M_\theta = \mp M_o \tag{7}$$

The upper signs refer again to the upper half of the yield curve. Each of these equations, by itself, can be easily solved for M_θ, and this value of M_θ substituted into the differential equation for M_r. The equations for M_r are then solved, and the procedure for solution can be continued. However, each straight-line portion of the yield curve has its own unique solution, and it must be determined exactly which regimes apply to each part of the plate at each instant of time. Four of the corners of the Tresca yield hexagon would also be plasticity regimes of finite width on the plate. Thus, although the differential equations are simplified, the solution of any specific plate problem involves keeping track, in time, of each boundary between different regimes of the solution. Even with this difficulty it appears that use of the Tresca yield condition offers a consistent, well-known approach for the general solution of plate problems in plasticity, and therefore it has been selected as the yield condition to use in the main analysis of this thesis.

Maximum reduced stress - Haythornthwaite.- This yield criterion was introduced some time ago (see ref. 40), but has not been extensively investigated as yet. Since this yield condition is a piecewise linear yield surface, a maximum statement for yielding is expected, and the yield surface can be written as

$$\max. \left\{ \left| \sigma_i - \sigma \right| \right\} - \frac{2}{3} \sigma_o = 0 \tag{8}$$

where σ is the average stress, or $\sigma = \frac{(\sigma_1 + \sigma_2 + \sigma_3)}{3}$. This six-sided surface is somewhat similar to the Tresca yield surface (see eq. (6)). For the case of plane stress ($\sigma_3 = 0$), equation (8) becomes a hexagon in the σ_1, σ_2 plane as shown in figure 3, and the equations for the sides become

$$(2\sigma_1 - \sigma_2) = \mp 2\sigma_o \qquad (2\sigma_2 - \sigma_1) = \pm 2\sigma_o \qquad \sigma_1 + \sigma_2 = \pm 2\sigma_o \qquad (9)$$

where again the upper signs refer generally to the upper half of the yield curve, and the lower signs to the lower half. Since these stresses are related directly to the moments, equation (9) is seen to yield linear relationships between the moments M_r and M_θ as in the case of Tresca yield criterion. However, from figure 3, it is seen that the Haythornthwaite yield condition closely circumscribes the von Mises ellipse, and can be used very effectively to provide, for example, an upper bound for load-carrying capacities of circular plates, while still retaining linear equations as in the Tresca yield condition. Also the Tresca yield condition can still be used effectively for a lower bound, and close approximation to actual load-carrying capacities can be obtained.

This yield condition also has additional advantages over the Tresca yield criterion in a few cases. The Tresca condition allows as many as three hinge circles to form (when considering the upper half of yield surface), but the Haythornthwaite condition allows only one hinge circle to form. These differences can cause a considerable variation in the computational effort required for a general solution. In the analysis

of a simply supported plate, however, the region of interest (shaded region A in fig. 2) is such that the Tresca yield criterion allows either one or two solution regimes, whereas the Haythornthwaite yield criterion always requires two regimes. For this reason, the Tresca yield condition is assumed in the main body of this dissertation.

Hinge Circles and Discontinuity Conditions

The term "hinge circle" and the definition of such a circle for plastic-plate problems can be directly traced to beam analyses that were conducted previously. Experimental results for beams (ref. 33) have verified that points occur along the beam across which a large change in the character of the deflection exists. The location of these points varies with time, and propagates along the beam in dynamic loading problems. In fact, the measured velocity of propagation of these "discontinuities" along the beam can be compared with the expected rate of propagation for the "hinges" that naturally occur in the rigid-plastic analysis of a beam. The calculated velocity of the hinge (using the Tresca yield criterion) agrees quite well with the experimental propagation rate except for very early times, and indicates that the rigid-plastic analysis yields reasonable results for a beam (see ref. 33).

Considering a generalization of this beam hinge concept for dynamically loaded circular plates, the term "hinge circle" was introduced to define the locations across the radius of the plate at which discontinuities in the circumferential curvature rate $-\frac{1}{r}\frac{\partial}{\partial t}\left(\frac{\partial w}{\partial r}\right)$ occur. These discontinuities have all of the appearances of hinges as in beams, and

again, experimental results (ref. 34) for plates generally verify the hinge propagation rates, even though the rigid-plastic theory yields infinite initial velocities under certain conditions. This agreement between experiment and rigid-plastic theory is somewhat surprising, since the material of the plate is inherently elastic, strain hardening, and under inplane and shear forces, etc., whereas the theory is derived for only the bending of a rigid-plastic material. This agreement in hinge circle motion implies that the bending theory gives a good estimate of plate motion until large deflections occur.

Since moving circles of discontinuity are a fundamental part of dynamic plastic-plate problems, a definition is needed for the changes in the solution as a discontinuity circle passes any given point. These changes are the so-called "jump conditions" of plastic-plate theory, and can be determined from the knowledge of the quantities which are continuous. For example, to retain integrity of the plate, the deflection w, as well as the plate velocity $\frac{\partial w}{\partial t}$, must be continuous everywhere in the plate, or

$$\left[w\right] = 0 \quad \text{and} \quad \left[\frac{\partial w}{\partial t}\right] = 0 \tag{10}$$

where the bracket denotes the difference in the variable enclosed in the bracket between one side of the circle of discontinuity and the other side. Thus, the bracket denotes the jump of its argument as a discontinuity passes. Now, if the location of the circle of discontinuity is defined as $\rho(t)$, this location can be plotted as in figure 5 as the

curve $r = \rho(t)$ in a rectangular r, t space. Moving along this curve, the rate of change of deflection may be written

$$\frac{dw}{ds} = \frac{\partial w}{\partial r}\frac{dr}{ds} + \frac{\partial w}{\partial t}\frac{dt}{ds} \tag{11}$$

Using the bracket notation presented in equation (10), the change of the quantities in equation (11) as the curve is crossed can be written

$$\left[\frac{dw}{ds}\right] = \left[\frac{\partial w}{\partial r}\right]\frac{dr}{ds} + \left[\frac{\partial w}{\partial t}\right]\frac{dt}{ds} \tag{12}$$

Since w is continuous along the curve, the left-hand side of equation (12) must be zero, and multiplication by $\frac{ds}{dt}$ yields

$$\left[\frac{\partial w}{\partial t}\right] + \left[\frac{\partial w}{\partial r}\right]\frac{d\rho(t)}{dt} = 0 \tag{13}$$

This equation shows the basic form of the discontinuity jump conditions for plastic-plate problems. Since $\left(\frac{\partial w}{\partial t}\right)$ is also continuous everywhere, equation (13) simplifies considerably. Also replacing w by $\frac{\partial w}{\partial t}$ in equation (13) yields another discontinuity condition; these two conditions can be written as

$$\frac{d\rho}{dt}\left[\frac{\partial w}{\partial r}\right] = 0 \tag{14}$$

$$\left[\frac{\partial^2 w}{\partial t^2}\right] + \frac{d\rho}{dt}\left[\frac{\partial^2 w}{\partial r\,\partial t}\right] = 0 \tag{15}$$

These two discontinuity conditions are consequences of maintaining the continuity of the plate (no breaking or plate failure). Dynamic equilibrium also requires that the moment M_r and the shear force Q_r be continuous in moving across a circle of discontinuity. By following the same procedure as for the deflections, the other two discontinuity conditions become:

$$\left[\frac{\partial M_r}{\partial t}\right] + \frac{d\rho}{dt}\left[\frac{\partial M_r}{\partial r}\right] = 0$$

$$\left[\frac{\partial Q_r}{\partial t}\right] + \frac{d\rho}{dt}\left[\frac{\partial Q_r}{\partial r}\right] = 0 \qquad (16)$$

In addition, for the case of a <u>moving</u> circle of discontinuity only, the only other second derivative jump condition can be written from equation (14). Since $\frac{d\rho}{dt}$ is nonzero, $\frac{\partial w}{\partial r}$ must be continuous, and therefore, from equation (13) directly

$$\left[\frac{\partial^2 w}{\partial r\, \partial t}\right] + \frac{d\rho}{dt}\left[\frac{\partial^2 w}{\partial r^2}\right] = 0 \qquad \left(\frac{d\rho}{dt} \neq 0\right) \qquad (17)$$

With all four of the basic jump conditions derived in general, in equations (14) through (16), the difference between moving and stationary discontinuities, and between hinge circles and nonhinge circles, becomes clear. If the discontinuity is not moving, then $\frac{d\rho}{dt}$ is zero, and all terms not containing $\frac{d\rho}{dt}$ must be continuous. Also, all bracketed terms that multiply $\frac{d\rho}{dt}$ terms may then have discontinuities at the circle.

If the circle of discontinuity is considered a hinge circle, then the terms containing $\frac{\partial^2 w}{\partial r\, \partial t}$ are nonzero, and the other terms that appear in conjunction with $\frac{\partial^2 w}{\partial r\, \partial t}$ must be discontinuous across the hinge circle.

In general, whenever a bracketed term can be shown to be zero across some circle of discontinuity, then its argument may be substituted into equation (13) for w, and another jump condition on higher derivatives can be written. The basic jump conditions, however, are still equations (14) through (16). With these general jump conditions then, the solutions in two different regimes may be related, and problems solved more readily. If a problem to be solved contained two circles of discontinuity, the jump conditions that would apply, if the two circles ever met, would have to be derived for the case of intersection of two curves of the same type as the single curve shown in figure 5. After two such curves intersect,a new solution must be initiated, and the resultant single curve that would apply after intersection would necessarily have a discontinuity in its slope at the intersection point. Such a discontinuity in velocity of propagation would be bothersome to analyze, but since this dissertation concerns only simply supported plates, only one circle of discontinuity is possible, and therefore, the difficulties caused by interfering circles are not present.

Plasticity Regimes

After selection of the yield criterion and the boundary conditions for any given problem, the yield curve and its associated flow rule must be applied for solution of the problem. Depending on the selections made, several possible regions (or "regimes") of solution can occur.

The solutions in each of these regimes must be matched at the circle of discontinuity between them, so that the continuity (and discontinuity) conditions of the previous section are satisfied. In this manner, the complete solution is found.

In the case of the von Mises yield criterion (see fig. 3), and for either simply supported or clamped boundary conditions, the plate is always in a single regime with uniquely defined normal directions. Therefore, the problems of different regimes of plasticity and solution matching at a circle of discontinuity are avoided. However, the nonlinear equations are generally not solvable in closed form, and numerical integration methods must be employed for solution.

All other yield curves discussed herein are piecewise linear, and various regimes of solution must be determined and matched. An additional difficulty also appears when the loading varies with time and radius. In very general cases, some regimes may appear and disappear as time increases. Therefore, proceeding to solutions in the general cases must be done slowly and carefully lest some regime of solution be improperly allowed or restricted. For piecewise linear yield curves, the linear portions of the curves are always possible regimes on the plate in the final solution. However, the corners of the yield curve may also be regimes of finite size, and each problem solved must be thoroughly analyzed for this possibility. Generally, it appears that a corner of the yield surface could represent a finite size regime on the plate only if that corner could possibly be a hinge circle. Indeed, if this is the case, then an estimate of the possible regimes for a given problem can be found simply

by the definition of a hinge circle as follows. Across a hinge circle, $\frac{\partial^2 w}{\partial r\, \partial t}$ is discontinuous by definition, and is directly related to the strain rate. In fact, at the outer fibers of the plate

$$\frac{\partial^2 w}{\partial r\, \partial t} = -\frac{r}{h}\,\dot{\epsilon}_\theta \tag{18}$$

If equation (1) is used at a hinge circle, then the normal to the yield curve has the direction cosines $(\dot{\epsilon}_\theta) : (\dot{\epsilon}_r)$. For unbounded $\dot{\epsilon}_\theta$, the normal to the yield curve must therefore have the possibility of being horizontal. Thus, all corners of the piecewise linear yield curves that admit the possibility of having a horizontal normal are possible finite regimes on the plate. From figures 3 and 4, for both simply supported and clamped plates, the possible finite corner regimes can then be read off directly: for Tresca, regimes A and D; for Johansen, regimes A and C; and for Haythornthwaite, none. Table I shows a listing of all the possible plasticity regimes for transversely loaded, circular plates considering all four yield criteria discussed herein. Whether all (or indeed any) of these regimes occur in any particular problem depends upon the manner and magnitude of the transverse loading, and care must be exercised in the process of solution.

Low Loading Cases - $p_o \leq p_{max.} \leq p_1$

As a general loading of sufficiently small magnitude is applied to a circular plate, the state of stress everywhere within the plate corresponds to a point inside of the yield curve, and for a rigid-plastic

material the plate must remain rigid. Irrespective of the type of loading and manner of application, the plate does not move or yield. As the magnitude of the loading increases, the plate has some states of stress corresponding to points closer to the yield curve, and, consequently, closer to yielding. As the magnitude of the loading increases still further, the state of stress at some location in the plate finally reaches a point on the yield curve and yielding starts. For a rigid-plastic material the stress is σ_o everywhere through the depth at that location, and the value of the loading that causes this yielding is defined as the "load-carrying capacity" of the plate. Since work hardening is neglected herein, all states of stress may not move beyond the original yield surface. The type of yielding that occurs and where it occurs is in the general case a function of the type of yield surface and the type of loading. In order to proceed further in this discussion, the Tresca yield condition for a plate with simply-supported edges is now assumed.

The load at which yielding starts and a hinge circle is first formed is defined as p_o. This value of loading is the load-carrying capacity for the Tresca yield criterion, which has been shown to yield a lower bound (ref. 40) for the actual load-carrying capacity of a plate with any general yield criterion. Thus, p_o can be used as a conservative estimate for design of rigid-plastic circular plates. For the Tresca yield criterion, the value of p_o is determined as follows: For initial yielding, a hinge circle (actually a point hinge) is formed at the origin of the circular plate. Then, $M_r = M_\theta = M_o$, and the center of the plate

is located at point A of the Tresca yield curve shown in figure 4. At the edge of the plate, the moment M_r is zero and point B of the yield curve applies. Therefore, the entire plate is in regime AB, the moment $M_\theta = M_o$ everywhere in the plate, and (neglecting the inertia term since the rigid regime is just ending) the differential equation for M_r becomes (see analysis section, eq. (39)),

$$\frac{\partial}{\partial r}(rM_r) - M_o = - \int_o^r q(r)p(t)r \, dr \tag{19}$$

If the time axis is shifted so that $t = 0$ corresponds to the initiation of motion, then $p(o) = p_o$. Solving equation (19) for M_r then yields (using the condition that $M_r = M_o$ at $r = 0$)

$$M_r = M_o - \frac{1}{r} p_o \int_o^r \left\{ \int_o^\eta q(r)r \, dr \right\} d\eta \tag{20}$$

Now, the boundary condition (that M_r at $r = b$ is zero) is applied, and p_o can be calculated as

$$p_o = \frac{bM_o}{\int_o^b q(r)r(b - r)dr} \tag{21}$$

This expression allows the calculation of the magnitude of $p(t)$, for which a general $q(r)$ loading will just cause a hinge to form. If the loading is considered to be uniform over either a circular region around

the origin or an annulus near the supports, the expressions for load-carrying capacity shown in reference 1 for such loadings are found.

For the problems analyzed herein, another quantity is also of interest. This quantity, called p_1, is defined as the magnitude of the time variation of loading (p(t)) above which the hinge circle on the plate must exist away from the origin. The determination of p_1 is a much more difficult problem than the determination of p_o, and it has not been calculated previously except for an impulsively applied uniform load (ref. 2). If the loading applied to a plate is increased above the value p_o, then inertia terms become important in the differential equation as the plate continues to deflect. However, the hinge remains at the center of the plate, and therefore the single regime AB still applies everywhere on the plate. As the load is increased, eventually the load p_1 is reached at which the distribution of moment M_r forces the hinge to move away from the origin. That is, below the load p_1, the moment $M_r = M_o$ at the origin and decreases monotonically with radius to zero at the supports. Above the load p_1, however, the moment just beyond the origin attempts to reach a value greater than M_o. Since the yield criterion precludes such a value, the hinge, therefore, must occur away from the origin.

The value of p_1 can be determined by solution of a general plasticity problem as follows: since the inertia force is important, the velocity must be determined in regime AB such that the velocity of the supports is zero. Thus, in regime AB, the curvature rate and support velocity are

$$\dot{\kappa}_r = -\frac{\partial^3 w}{\partial r^2 \partial t} = 0 \qquad \left.\frac{\partial w}{\partial t}\right|_{r=b} = 0 \tag{22}$$

Integrating twice with respect to r and using the boundary velocity equal to zero, the velocity can be calculated from equations (22) as

$$\frac{\partial w}{\partial t} = C_1(t)(r - b) \tag{23}$$

The differential equation for the moment M_r in regime AB (with $M_\theta = M_o$) is written (from the analysis section, eq. (39)) as

$$\frac{\partial}{\partial r}(rM_r) - M_o = -\int_o^r \left[q(r)p(t) - \mu \frac{\partial^2 w}{\partial t^2}\right] r\, dr \tag{24}$$

Substituting the plate velocity from equation (23) into equation (24), and solving, the moment M_r becomes

$$M_r = M_o - \frac{p(t)}{r} \int_o^r \left\{\int_o^\eta q(\xi)\xi\, d\xi\right\} d\eta + \frac{\mu \dot{C}_1}{r} \int_o^r \left\{\int_o^\eta (\xi - b)\xi\, d\xi\right\} d\eta + \frac{C_3}{r} \tag{25}$$

Two boundary conditions must be satisfied on M_r. These are

$$M_r\big|_{r=0} = M_o \quad \text{and} \quad M_r\big|_{r=b} = 0 \tag{26}$$

To apply the boundary condition at $r = 0$, the two integral terms in equation (25) must be evaluated using L'Hospital's rule and Leibniz' rule for differentiation under an integral sign. Thus, for example,

$$\lim_{r \to 0} \frac{\int_o^r \left\{ \int_o^\eta q(\xi)\xi \, d\xi \right\} d\eta}{r} = \lim_{r \to 0} \frac{\int_o^r q(\xi)\xi \, d\xi}{(1)} = 0 \qquad (27)$$

In this manner, both of the integral terms vanish, and application of the first boundary condition yields $C_3 = 0$. Application of the second boundary condition is direct, and yields

$$\mu \dot{C}_1 = \frac{-bM_o + p(t) \int_o^b \left\{ \int_o^\eta q(\xi)\xi \, d\xi \right\} d\eta}{\left(\frac{-b^4}{12} \right)} \qquad (28)$$

Therefore, M_r is fully known. Calculation of the derivative of M_r follows directly from equations (25) and (28), and is

$$\frac{\partial M_r}{\partial r} = p(t) \left\{ \frac{1}{r^2} \int_o^r \left\{ \int_o^\eta q(\xi)\xi \, d\xi \right\} d\eta - \frac{1}{r} \int_o^r q(\xi)\xi \, d\xi \right\} + \left\{ \frac{12M_o}{b^3} \right.$$

$$\left. - p(t)\frac{12}{b^4} \int_o^b \left\{ \int_o^\eta q(\xi)\xi \, d\xi \right\} d\eta \right\} \left\{ - \frac{1}{r^2} \int_o^r \left\{ \int_o^\eta (\xi \right. \right.$$

$$\left. \left. - b)\xi \, d\xi \right\} d\eta + \frac{1}{r} \int_o^r (\xi - b)\xi \, d\xi \right\} \qquad (29)$$

By simultaneous application of L'Hospital's rule and Leibniz' rule, all of the terms in equation (29) become zero as r approaches zero.

Therefore, the origin is an extremum point for the moment. To determine whether the origin is actually a maximum point (as required by the yield criterion) or not, the second derivative of the moment must be evaluated at the origin. Again, the same method is applied, and at the origin the second derivative becomes

$$\left.\frac{\partial^2 M_r}{\partial r^2}\right|_{r=0} = -p(t)\frac{q(o)}{3} + \frac{4}{b^3}\left(-bM_o + p(t)\int_o^b \left\{\int_o^\eta q(\xi)\xi\, d\xi\right\} d\eta\right) \tag{30}$$

This expression changes sign from minus to plus at a value of $p(t)$ equal to p_1, and equating expression (30) to zero yields

$$p_1 = \frac{bM_o}{\int_o^b q(\xi)\xi(b - \xi)d\xi - \frac{q(o)b^3}{12}} \tag{31}$$

For values of loading less than this value, the moment curve has a true maximum at the origin. For values of loading greater than p_1, this moment distribution would increase with r from its value of M_o at the origin. Such an increase would violate the yield criterion and cannot be allowed. In such cases, the hinge circle moves outward from the origin, causing a finite region of regime A to appear, and the difficulties of a moving hinge circle must be surmounted.

High Loading Cases - $p_{max.} > p_1$

If the maximum loading applied to the plate is less than p_1, then the actual variation of the loading can be analyzed directly. This is due to the fact that the hinge circle remains at the origin, and a single regime (AB) applies to the entire plate. For higher values of the loading, however, the hinge circle exists away from the origin and the actual shape of the loading is of prime importance. While the term "time varying loading" can refer, in general, to any variation with time, this term is restricted herein to loadings containing a single peak, that is, an initial increase in loading followed by a decay toward zero. This restriction is applied for several reasons. As mentioned previously, the main problems of interest to dynamic plasticity for circular plates are impact and ballistic problems, in which the loading is expected to have a single peak. In fact, estimation of the contact force experimentally (ref. 41) by photographic means for a ballistic problem indicated that the force varied as

$$F = F_o t^2 e^{-\beta t} \tag{32}$$

In addition, an excellent discussion of theoretical analyses of such ballistic problems (ref. 39) indicated that the method developed by Karas (ref. 42) also yields reasonable results for ballistic problems. Essentially, this approach assumed that a simply supported rectangular elastic plate was impacted by a spherical elastic projectile. Considering a Hertzian type of elastic impact, a difficult integral equation was

derived for the contact force history between the two elements and solved numerically. The numerical results for a specific case (20 cm by 20 cm steel plate with a thickness of 0.8 cm impacted by a 2 cm radius steel sphere) with a very low 1 meter/sec velocity, showed a response similar to equation (32). The magnitude of the maximum applied force was high (320 lb) and the duration of the loading was very small (12.8 μ-sec). These values are quite surprising, since the velocity and mass of the projectile are small, and the resultant loading on the plate appears large. These results lend support to the often-applied assumptions that the loading starts at a maximum value and decreases rapidly. In any case, the theoretical results agree with the experimental results in predicting at most a single maximum peak. A short general discussion of both the increasing and decreasing phases of loading is given in the next two sections.

Increasing loading above p_1.- In this case, the plate has initial conditions determined from the solution with the hinge circle fixed at the origin as mentioned in the section entitled Low Loading Cases. Increasing the loading above p_1 causes the hinge circle to move outward on the plate in a continuous manner. If the loading is allowed a discontinuity in time (such as an impulsive jump in loading), then all variables for the problem $\left(\text{except } w \text{ and } \frac{\partial w}{\partial t} \text{ as required by continuity of the plate}\right)$ can have discontinuities. The initial location of the hinge circle (ρ_o) can, therefore, be nonzero for a large initial impulse in loading. However, once the hinge has moved away from the origin, it

may not have a discontinuous jump in position thereafter. This fact can be shown directly from the jump conditions derived previously.

Therefore, it might be helpful to assume that as the loading increases, the hinge would move outward at a calculable rate, until it reaches a maximum value, after which it monotonically decreases toward the origin. Whether this is actually the case or not depends on the shape of both the radial and time variations of loading. There is the possibility that the shapes of these loadings may cause the hinge to move outward and inward several times before reaching the origin. If this is the case, great difficulty arises, for example, in determination of deflections, since the velocity expressions in the different regimes must be integrated for as long a time as they apply to any particular point. Finally, the yield surface restrictions on curvature rates (greater than or equal to zero in regime A) may preclude solution for some loading conditions. A discussion of this possibility follows equation (47).

Decreasing loading below $p_{max.}$.- In this case, many of the accompanying difficulties of the previous section apply. As the loading is reduced, in general, the hinge may move inward or outward, and its exact location is important. For the case of a loading that is suddenly removed (see ref. 2), the hinge circle has been shown to decrease monotonically to the origin. If the loading is removed relatively quickly, then, it is reasonable to expect that the hinge will still move continually toward the origin. However, only careful solution of the hinge circle movement equation will tell how the hinge circle moves.

BASIC ASSUMPTIONS

In the solution of any general problem in plasticity a number of assumptions are needed to allow analytical solutions to be written. Some of the assumptions stated in this section have been discussed in earlier sections and will only be mentioned briefly for completeness. General discussion of these basic assumptions is available in references 1 through 6. There are three general types of assumptions necessary for solution: assumptions on constitutive equations, assumptions on deformations to be allowed, and geometrical assumptions required for the problem of interest.

The material of the plate is assumed to be rigid-perfectly plastic. Rigid-perfectly plastic theory disallows the inclusion of work-hardening effects. Inclusion of work-hardening would necessitate a continually changing yield surface to be allowed, and the conditions for yielding would soon vary with the location on the plate and time, creating severe difficulties for solution. The material of the plate is also assumed to follow the Tresca yield criterion, which is a maximum shearing stress criterion (see fig. 4). Considering the boundary conditions to be only simply supported, the two regimes that apply are A and AB (see table 1), and the flow rules associated with these regimes define the strain-rate ratios from the normals to the yield surface as

$$\begin{aligned} &\text{Regime } \underline{A} \qquad \dot{\epsilon}_r:\dot{\epsilon}_\theta = 1 - \beta:\beta \qquad (0 \le \beta \le 1) \\ &\text{Regime } \underline{AB} \qquad \dot{\epsilon}_r:\dot{\epsilon}_\theta = 0:1 \end{aligned} \tag{33}$$

These flow rules allow solution for the deflections in many cases and are often applied most effectively by means of curvature rates. Assuming that

normals to the original middle surface of the plate remain normal to the deformed middle surface, the strain rates throughout the plate depth are directly related to the curvature rates of the middle surface. In fact, the strain rates through the depth are

$$\dot{\epsilon}_r = \frac{\partial \dot{u}}{\partial r} = -z \frac{\partial^3 w}{\partial r^2 \partial t} \quad \text{and} \quad \dot{\epsilon}_\theta = \frac{\dot{u}}{r} = -z \frac{1}{r} \frac{\partial^2 w}{\partial r \partial t} \tag{34}$$

and the curvature rates of the middle surface are

$$\dot{\kappa}_r = -\frac{\partial^2 \dot{w}}{\partial r^2} \quad \text{and} \quad \dot{\kappa}_\theta = -\frac{1}{r} \frac{\partial \dot{w}}{\partial r} \tag{35}$$

so that

$$\dot{\epsilon}_r : \dot{\epsilon}_\theta = \dot{\kappa}_r : \dot{\kappa}_\theta \tag{36}$$

It is also seen that the stress at each value of z must be at the yield condition for the plate to bend. Therefore, the stress above the middle surface of the plate is defined by one point on the yield surface, and the stress below the middle surface of the plate is defined by the diametrically opposite point on the yield surface. In this manner, the moments and stresses are related as

$$M_r = \int_{-h}^{+h} \sigma_r z \, dz = \sigma_r \int_{-h}^{o} z \, dz + \sigma_r \int_{o}^{+h} z \, dz = \sigma_r h^2 \tag{37}$$

This stress distribution is discontinuous at the middle surface, but such a discontinuity is allowable for rigid-plastic theory.

The plate is also assumed to be axisymmetric with respect to both loading and boundary conditions. This is a usual assumption for circular plate problems, and leads to the very desirable result of removing the shear stresses $\tau_{r\theta}$ and $\tau_{\theta z}$ identically. The twisting moments $M_{r\theta}$ and the shear force Q_θ resulting from these stresses likewise vanish. If the plate is considered thin, then the vertical stress σ_z and the shearing stress τ_{rz} can be considered, on the whole, to be small in comparison to the bending stresses σ_r and σ_θ. This is the usual bending theory for plastic plates and should be applicable for initial deflections under dynamic loading. If membrane forces were allowed, then as soon as deflection started, additional load would be required to continue the deflection and, instead of allowing only bending moments to affect the yield surface, the inplane forces N_r and N_θ would have to be included. A four-dimensional yield surface would then be necessary with an appropriate theory for interaction between these quantities at yield (see ref. 11). Such a generalization herein would obscure the desired insight into general plastic plate problems and is not included. Similarly, shearing deformation of the plate is neglected. This assumption is valid if the loaded surface of the plate extends over a region of the plate that is large compared to the thickness. In view of the allowance herein of rather general radial load distributions, the application to concentrated loads is not made here. One final assumption is also made, that the loading on the surface of the plate is separable into radial and time functions, so that the influence of both effects can be investigated separately. With these basic assumptions, then, the analysis can proceed directly to evaluate the influence of load distribution.

ANALYSIS

Under the basic assumptions of the previous section, a typical plate element is shown in figure 6 with the applied forces and moments. In addition to the principal bending moments and shear force, the plate has a general surface loading $q(r)p(t)$ and a resisting inertia force as well.

Basic Equations

From the plate element shown in figure 6, the basic differential equations can be derived. Taking the summation of forces and moments, and neglecting higher order differentials, these equations become

$$\frac{\partial}{\partial r}(rQ_r) + rq(r)p(t) = \mu r \frac{\partial^2 w}{\partial t^2}$$

$$\frac{\partial}{\partial r}(rM_r) - M_\theta = rQ_r \tag{38}$$

where μ represents the mass density per unit area of the plate middle surface. The shear force is eliminated from these two equations to yield one differential equation for the moments.

$$\frac{\partial}{\partial r}(rM_r) - M_\theta = -\int \left[q(r)p(t) - \mu \frac{\partial^2 w}{\partial t^2}\right] r \, dr \tag{39}$$

For a simply supported plate, the moments M_r and M_θ are equal at the center of the plate, and at the boundary the moment M_r is zero. Therefore, from the Tresca yield condition (see fig. 4) the center of the plate

corresponds to point A on the yield surface, and the edge of the plate corresponds to the point B. Since B cannot be a plasticity regime (table 1), at most a central region of regime A and an outer annular region of regime AB exist, separated by a hinge circle located at $r = \rho(t)$. The differential equation (39) must then be appropriately solved in each regime. The moment M_θ is constant between points A and B of the Tresca yield hexagon, and consequently, it has been replaced by M_o in the following sections.

Solution - Regime A

In this regime, $M_r = M_o$ and the differential equation (39) reduces to

$$p(t)\int_o^r q(r)r\,dr - \mu\int_o^r \frac{\partial^2 w}{\partial t^2}\,r\,dr = 0 \tag{40}$$

To solve this equation for the "deflection rate" $\partial w/\partial t$, a separation of variables solution is written, so that

$$\frac{\partial w}{\partial t} = q(r)R(r)T(t) \tag{41}$$

Substituting this expression into equation (40) and separating the radial and time variables yields

$$\frac{\mu}{p(t)}\frac{dT(t)}{dt} = C = \frac{\int_o^r q(r)r\,dr}{\int_o^r q(r)R(r)r\,dr} \tag{42}$$

where C is a constant of separation. Solving these equations for the T(t) and R(r) expressions,

$$T(t) = \frac{C}{\mu} \int p(t)dt \tag{43}$$

$$\int_o^r R(r)q(r)r\,dr = \frac{1}{C} \int_o^r q(r)r\,dr \tag{44}$$

Taking the derivative of equation (44) with respect to r (or by inspection), $R(r)$ is seen to be simple $\frac{1}{C}$. Substitution of this value and equation (43), both into equation (41), the deflection rate in this regime is found to be

$$\frac{\partial w}{\partial t} = \frac{q(r)}{\mu} \int p(t)dt \tag{45}$$

Since the moments are already known, the solution is then complete. If the deflections are desired, then equation (45) must be integrated with respect to time. If the strain rates are desired, equation (45) must be differentiated with respect to r. Equation (45) shows the important fact that the velocity distribution in the interior region follows the radial distribution of the loading. This fact has generally been listed as an assumption previously, although only uniform radial load distributions have been investigated extensively.

This expression has several restrictions on its applicability; for example, it applies only for $r \leq \rho(t)$. If the loading increases in time to a peak and then decreases, the equation (45) does not apply until $p > p_1$ (defined in a previous section), since below p_1 regime A does not exist. When $p > p_1$, the regime A exists until the hinge circle

shrinks back to a point at the origin. This time must be determined directly from solution of the equation for hinge circle motion. Both before and after regime A appears, the hinge remains at the origin for a finite length of time. Otherwise, the plate remains rigid. Thus, the limits of integration in equation (45) are not directly defined. This is the basic difficulty caused by hinge circle movement.

The flow rule also must apply in regime A. From equations (33) and (35), the flow rule in this regime states that

$$\dot{\kappa}_r = -\frac{\partial^3 w}{\partial r^2 \partial t} = -\frac{1}{\mu}\frac{\partial^2 q(r)}{\partial r^2}\int p(t)dt \geq 0$$

and (46)

$$\dot{\kappa}_\theta = -\frac{1}{r}\frac{\partial^2 w}{\partial r \partial t} = -\frac{1}{\mu r}\frac{\partial q(r)}{\partial r}\int p(t)dt \geq 0$$

Since $p(t)$ and $q(r)$ are considered only positive quantities, then in regime A the following restrictions on radial load distribution must apply:

$$\frac{\partial^2 q(r)}{\partial r^2} \leq 0 \quad \text{and} \quad \frac{\partial q(r)}{\partial r} \leq 0 \tag{47}$$

If the loading under investigation does not meet these restrictions, then two possibilities exist. Either regime A does not ever exist in that problem, or the present approach is inapplicable. It appears most logical to assume the plate remains entirely in regime AB, and for some cases that have been analyzed, this was the case. Finally, it must be mentioned that the jump conditions between regimes A and AB across the hinge circle ρ must still be satisfied.

Solution - Regime AB

Obtaining the solution in this regime is easier if the velocity expression $\partial w/\partial t$ is found first. Then, the acceleration term can be evaluated in the moment equation, and the moment M_r can be calculated directly. To determine the velocity distribution, the flow rule must be applied. In this regime, this is simply

$$\dot{\kappa}_r = - \frac{\partial^3 w}{\partial r^2 \partial t} = 0 \tag{48}$$

Solution of this equation for the velocity can be accomplished directly by separation of variables. With consideration for the requirement that the solution for velocity must be continuous across the hinge circle $r = \rho(t)$, the general solution will be written instead as

$$\frac{\partial w}{\partial t} = q(\rho) f_1(r,\rho,t) \tag{49}$$

Substitution of this equation into equation (48) yields a differential equation for $f_1(r,\rho,t)$ with the solution

$$f_1(r,\rho,t) = rC_1(\rho,t) + C_2(\rho,t) \tag{50}$$

Realizing that the velocity must be zero at the supports ($r = b$), the functions $C_1(\rho,t)$ and $C_2(\rho,t)$ must be related as follows:

$$C_2(\rho,t) = -bC_1(\rho,t) \tag{51}$$

Now, the velocity must be continuous across the hinge circle $r = \rho(t)$, and the velocities in both regimes are

Regime A
$$\frac{\partial w}{\partial t} = \frac{q(r)}{\mu} \int p(t)dt$$

Regime AB
$$\frac{\partial w}{\partial t} = q(\rho)(r - b)C_1(\rho,t) \qquad (52)$$

Equating these two velocity expressions at $r = \rho$ yields $C_1(\rho,t)$ as

$$C_1(\rho,t) = \frac{1}{\mu(\rho - b)} \int p(t)dt \qquad (53)$$

Substitution of equations (50), (51), and (53) back into equation (49) yields, finally, the velocity distribution in regime AB

$$\frac{\partial w}{\partial t} = \frac{q(\rho)(r - b)}{\mu(\rho - b)} \int p(t)dt \qquad (54)$$

This velocity expression for regime AB only applies for r greater than $\rho(t)$. It is seen to be linear in r, so that the outer annulus of the plate deforms into a conical shape even in the general case. When the initial loading on the plate is less than p_o, the plate remains rigid. Otherwise, regime AB applies for some region on the plate until motion ceases. The strain rate and deflection can be calculated directly from equation (54) by differentiation and integration, and the solution can be completed in this regime by determination of the moment M_r. The expression for the acceleration term $\partial^2 w/\partial t^2$ is

$$\frac{\partial^2 w}{\partial t^2} = \frac{(r - b)}{\mu(\rho - b)}\left[p(t)q(\rho) + \frac{d\rho}{dt}\left(\frac{\partial q(\rho)}{\partial \rho} - \frac{q(\rho)}{(\rho - b)}\right)\int p(t)dt\right] \tag{55}$$

and substitution of this expression into equation (39) yields the differential equation to solve for M_r. Note the rate of hinge circle motion ($d\rho/dt$) appears and must be evaluated. Solution of the equation for M_r (eq. (39)) yields

$$M_r = \frac{-I_2(\rho,r)}{r(\rho - b)}\left[p(t)q(\rho) + \frac{d\rho}{dt}\left(\frac{\partial q(\rho)}{\partial \rho} - \frac{q(\rho)}{(\rho - b)}\right)\int p(t)dt\right]$$
$$+ \frac{(r - \rho)}{r} M_o - \frac{p(t)}{r} I_1(\rho,r) + \frac{C_3(\rho,t)}{r} \tag{56}$$

where

$$I_1(\rho,r) = \int_\rho^r \left\{\int_\rho^\eta q(\xi)\xi \, d\xi\right\} d\eta \tag{57}$$

and

$$I_2(\rho,r) = \int_\rho^r \left\{\int_\rho^\eta (b - \xi)\xi \, d\xi\right\} d\eta \tag{58}$$

These integral expressions are rather involved, but can be reduced to single integrals by interchanging the order of integration, and integrating. In general, interchange of order can be written for integrals of this type as

$$\int_\rho^r \left\{\int_\rho^\eta g(\xi,\eta)d\xi\right\} d\eta = \int_\rho^r \left\{\int_\xi^r g(\xi,\eta)d\eta\right\} d\xi \tag{59}$$

and since the integrands in equations (57) and (58) are not functions of η, they can be integrated. In this manner, these integrals become

$$I_1(\rho,r) = \int_{\rho}^{r} q(\xi)\xi(r - \xi)d\xi \tag{60}$$

$$I_2(\rho,r) = \int_{\rho}^{r} (b - \xi)\xi(r - \xi)d\xi = \frac{br}{2}(r^2 - \rho^2)$$

$$- \frac{(r + b)}{3}(r^3 - \rho^3) + \frac{(r^4 - \rho^4)}{4} \tag{61}$$

Two functions still remain undefined, $C_3(\rho,t)$ and $d\rho/dt$. However, the moment M_r has two boundary conditions to be satisfied, and these are

$$M_r\Big|_{r=b} = 0 \quad \text{and} \quad M_r\Big|_{r=\rho} = M_o \tag{62}$$

If it is realized from equations (60) and (61) that when $r = \rho$ both integrals are zero, the second of these boundary conditions yields $C_3(\rho,t)$ as

$$C_3(\rho,t) = \rho M_o \tag{63}$$

Application of the first of boundary conditions (62) yields the differential equation to solve for $\rho(t)$. This equation is discussed in the next section and will not be discussed here. However, the expression for M_r contains $d\rho/dt$ and, using the $d\rho/dt$ equation, this term can be eliminated. After much algebraic manipulation, the moment expression can be written

$$M_r = M_o - \frac{bM_oI_2(\rho,r)}{rI_2(\rho,b)} - \frac{p(t)}{r}\left\{I_1(\rho,r) - I_1(\rho,b)\frac{I_2(\rho,r)}{I_2(\rho,b)}\right\} \tag{64}$$

Therefore, once the location of the hinge circle is known, the moment can be calculated, as well as the velocity from equation (54), and the solution for regime AB is complete.

Hinge Circle Movement

Consideration of the manner in which the hinge circle moves across the plate is a prime requirement for the solution of dynamic plasticity problems for thin plates. The rate at which the hinge circle moves can be defined from the moment expression in regime AB, as mentioned previously. That is, equation (56) for the radial moment (with $C_3(\rho,t) = \rho M_o$) must be set equal to zero at the supports ($r = b$). This expression is then solved for the hinge velocity $d\rho/dt$ and yields

$$\frac{d\rho}{dt} = \frac{bM_o - p(t)\rho_1}{\left\{\int p(t)dt\right\}\rho_2} \tag{65}$$

where

$$\rho_1 = I_1(\rho,b) + \frac{q(\rho)}{(\rho - b)} I_2(\rho,b)$$

and

$$\rho_2 = \left\{\frac{\partial q(\rho)}{\partial \rho} - \frac{q(\rho)}{(\rho - b)}\right\} \frac{I_2(\rho,b)}{(\rho - b)}$$

Now, the basic manner of hinge circle movement can be discussed.

The basic question of whether the hinge circle moves inward or outward depends on the sign of $d\rho/dt$. The time functions shown are all positive, but the ρ functions can have either sign and can cause the hinge to move in any direction. The integrals $I_1(\rho,b)$ and $I_2(\rho,b)$

are both only positive, but ρ_1 is negative only if

$$I_1(\rho,b) < \frac{q(\rho)}{(b - \rho)} I_2(\rho,b) \tag{66}$$

and ρ_2 is negative only if

$$\frac{1}{(\rho - b)} \frac{\partial q}{\partial \rho} < \frac{q(\rho)}{(\rho - b)^2} \tag{67}$$

The four quantities shown above are all positive, but their magnitudes may cause the hinge to move inward or outward depending on the shape of the $q(r)$ function selected. The only possibility that exists in the general case is to use a computer to solve for $\rho(t)$. A computer program to solve equation (65) for any general functions $q(r)$ and $p(t)$ has been written and a listing of the program is presented in the appendix.

Exact solution of equation (65) is possible in only two general cases. The variables in the equation are directly separable whenever either $p(t)$ or ρ_1 are zero or constant. When no loading is applied to the plate, $p(t)$ is always zero and a trivial case exists, but when $p(t)$ becomes zero after a finite length of time, then the motion of the hinge circle can be exactly calculated from that point onward. The function $p(t)$ could also be zero in one other very important case. That case is any general impulsive loading, in which $p(t)$ is defined as zero, but the integral of $p(t)$ is defined as a finite impulse applied to the plate. This general class of problems is very important, and a later section is devoted to the impulsive loading problem. The condition that $p(t)$ is a constant occurs if the load is applied as $p(> p_o)$ and

remains on the plate. Then, a fixed hinge circle problem is to be solved and equation (65) is not needed.

The case in which ρ_1 is a constant can be determined directly as follows. The function $q(\rho)$ must be found that makes the following equation true:

$$\rho_1 = \int_{\rho}^{b} q(\xi)\xi(b - \xi)d\xi - \frac{q(\rho)}{12}(b - \rho)^2(b + 3\rho) = C \qquad (68)$$

Taking the derivative of this equation with respect to ρ and combining terms yields

$$(b - \rho)\frac{dq(\rho)}{d\rho} = -q \qquad (69)$$

Solution of this equation shows that the distribution under discussion is

$$q(r) = C(b - r) \qquad (70)$$

This is a triangular loading case and would allow the differential equation on ρ to be separable. However, for this loading distribution, the hinge must only occur at the origin, and equation (65) is inapplicable anyway. The deflection of the plate is conical in both regimes, and the definition of the hinge circle breaks down in this case. Due to all these difficulties, the triangular loading case is not considered herein.

Matching Solutions at the Hinge Circle

The solutions on both sides of the hinge circle must satisfy the jump conditions derived in a previous section for hinge circles. These jump conditions can be written out and proven to be satisfied in general.

Difficulty is caused only by the impossibility of satisfying the $d\rho/dt$ equation exactly for all cases. However, some of the jump conditions are seen to be identically satisfied. For example, in the process of determining the solution in regime AB, the continuity conditions (eqs. (10)) were applied to yield the solution. Therefore, these conditions are identically satisfied. However, when a jump condition is found to include jumps in quantities that contain only derivatives with respect to r, this jump condition is much more difficult to evaluate in the general case. To express derivatives with respect to r only, the velocity expressions must be integrated with respect to t to determine deflections, and then the deflections must be differentiated with respect to r. The integration on time is necessarily a function of location; that is,

<u>in regime A only</u>

$$w(r,t) = \int_{t_o}^{t(\rho)} \frac{\partial w(r,t)}{\partial t}\, dt = \int_{t_o}^{t(\rho)} \left\{ \frac{q(r)}{\mu} \int p(t)dt \right\} dt \qquad (71)$$

$r <$ least ρ value

<u>in regime AB only</u>

$$w(r,t) = \int_{t_o}^{t(\rho)} \frac{\partial w(r,t)}{\partial t}\, dt = \int_{t_o}^{t(\rho)} \left\{ \frac{q(\rho)(r - b)}{\mu(\rho - b)} \int p(t)dt \right\} dt$$

$r >$ greatest ρ value

<u>in regime A then AB-inward moving hinge</u>

$$w(r,t) = \int_{t_o}^{t(r)} \left\{ \frac{q(r)}{\mu} \int p(t)dt \right\} dt + \int_{t(r)}^{t(\rho)} \left\{ \frac{q(\rho)(r - b)}{\mu(\rho - b)} \int p(t)dt \right\} dt$$

$\rho \leq r < \rho_o$

in regime AB then A-outward moving hinge

$$w(r,t)\int_{t_o}^{t(r)}\left\{\frac{q(\rho)(r-b)}{\mu(\rho-b)}\int p(t)dt\right\}dt+\int_{t(r)}^{t(\rho)}\left\{\frac{q(r)}{\mu}\int p(t)dt\right\}dt$$

$$\rho_o < r \leq \rho$$

where $t(\rho)$ is the time at which the hinge circle has moved to its current location, and $t(r)$ is the time at which the hinge circle first reached the point r. These functions, as well as the functions of ρ that occur under the integral sign, must be determined from the solution of the hinge circle movement (eq. (65)) as functions of time to yield deflections. Now, if the jump conditions on radial derivatives are to be written at the hinge circle, the deflections at points adjacent to the hinge must be written. If the hinge has only moved outward, then the deflection on the inside of the hinge circle is expressed as the last of equations (71), and the deflection on the outside of the hinge circle is the second of equations (71). If the hinge only moved inward, then the other two of equations (71) would apply. For an outward moving hinge, the jump in $\partial w/\partial r$ when passing from the inside to the outside of the hinge is

$$\left[\frac{\partial w}{\partial r}\right]=\int_{t_o}^{t(r)}\left\{\frac{q(\rho)}{\mu(\rho-b)}\int p(t)dt\right\}dt+\int_{t(r)}^{t(\rho)}\left\{\frac{\partial q(r)}{\partial r}\int\frac{p(t)dt}{\mu}\right\}dt$$

$$+\frac{dt(r)}{dr}\frac{(r-b)}{\mu(\rho-b)}q(\rho)\int p(t)dt\Big|_{t=t(r)}-\frac{dt(r)}{dr}\frac{q(r)}{\mu}\int p(t)dt\Big|_{t=t(r)}$$

$$-\int_{t_o}^{t(\rho)}\left\{\frac{q(\rho)}{\mu(\rho-b)}\int p(t)dt\right\}dt \qquad (72)$$

If $r = \rho$ all the integral terms cancel directly, and all dt/dr terms (when multiplied by $d\rho/dt$) also cancel, satisfying the jump condition (14). For the other case of an inward moving hinge, the same equation (72) is identically found. If the hinge moved inward and outward several times, then each time it passed a given point r another integral factor would have to be added to the deflection expressions to denote the change in regime. However, the jump condition on $\partial w/\partial r$ is directly satisfied whether the hinge moves either inward or outward. Also, the jump condition on $\partial^2 w/\partial r^2$ can be proven, in general, by carefully differentiating equation (72) and letting $r = \rho$ for both inward and outward moving hinges.

The jump condition of equation (15) can be verified, in the general case of a moving hinge circle, by means of the velocity expressions already derived in both regimes. Consider the jump as the magnitude when passing from the inside to the outside of the hinge circle, then

$$\left[\frac{\partial^2 w}{\partial r \partial t}\right] = \frac{\partial q(r)}{\partial r} \int \frac{p(t)dt}{\mu} - \frac{q(\rho)}{(\rho - b)} \int \frac{p(t)dt}{\mu}\Bigg|_{r=\rho} \tag{73}$$

and

$$\left[\frac{\partial^2 w}{\partial t^2}\right] = \frac{q(r)}{\mu} p(t) - \frac{q(\rho)(r - b)}{\mu(\rho - b)} p(t)$$

$$- \frac{(r - b)}{\mu} \int p(t)dt \left\{\frac{-q(\rho)}{(\rho - b)^2} + \frac{1}{(\rho - b)} \frac{\partial q(\rho)}{\partial \rho}\right\} \frac{d\rho}{dt}\Bigg|_{r=\rho} \tag{74}$$

Now, multiply equation (73) by $d\rho/dt$ and add to equation (74), letting $r = \rho$, so that the jump condition becomes

$$\frac{q(\rho)}{\mu}\,p(t) - \frac{q(\rho)(\rho-b)}{\mu(\rho-b)}\,p(t) - \frac{(\rho-b)}{\mu}\int p(t)dt\,\frac{d\rho}{dt}\left\{\frac{-q(\rho)}{(\rho-b)^2} + \frac{1}{(\rho-b)}\,\frac{\partial q(\rho)}{\partial\rho}\right\}$$

$$+\frac{d\rho}{dt}\left\{\frac{\partial q(\rho)}{\partial\rho}\int\frac{p(t)dt}{\mu} - \frac{q(\rho)}{(\rho-b)}\int\frac{p(t)dt}{\mu}\right\} = 0 \qquad (75)$$

By close inspection of equation (75), it can be seen that all terms are canceled by similar terms and this jump condition is identically satisfied.

The jump condition on moment M_r can also be easily verified in the general case. Since $M_r = M_o$ in regime A, the jump condition (eq. (16)) defines the value of the derivatives of M_r in regime AB as the hinge circle is approached. Then, in regime AB (eq. (64))

$$\frac{\partial M_r}{\partial r} = -\frac{bM_o}{I_2(\rho,b)}\left(\frac{1}{r}\,\frac{\partial I_2(\rho,r)}{\partial r} - \frac{I_2(\rho,r)}{r^2}\right) - p(t)\left\{\frac{1}{r}\,\frac{\partial I_1(\rho,r)}{\partial r}\right.$$

$$\left. - \frac{I_1(\rho,r)}{r^2} - \frac{I_1(\rho,b)}{I_2(\rho,b)}\left(\frac{1}{r}\,\frac{\partial I_2(\rho,r)}{\partial r} - \frac{1}{r^2}\,I_2(\rho,r)\right)\right\} \qquad (76)$$

and

$$\frac{\partial M_r}{\partial t} = -\frac{bM_o}{r}\left(\frac{I_2(\rho,b)\,\dfrac{\partial I_2(\rho,r)}{\partial\rho} - I_2(\rho,r)\,\dfrac{\partial I_2(\rho,b)}{\partial\rho}}{\left\{I_2(\rho,b)\right\}^2}\right)\frac{d\rho}{dt} - \frac{p(t)}{r}\,\frac{d\rho}{dt}\left\{\frac{\partial I_1(\rho,r)}{\partial\rho}\right.$$

$$\left. - \frac{\partial}{\partial\rho}\,\frac{I_1(\rho,b)I_2(\rho,r)}{I_2(\rho,b)}\right\} - \frac{1}{r}\,\frac{\partial p(t)}{\partial t}\left\{I_1(\rho,r) - \frac{I_1(\rho,b)I_2(\rho,r)}{I_2(\rho,b)}\right\} \qquad (77)$$

Noting that $I_1(\rho,r) = I_2(\rho,r) = 0$ as r approaches ρ, and that adding equation (77) to $d\rho/dt$ times equation (76) should yield zero (the jump condition), then

$$- \frac{bM_o}{\rho I_2(\rho,b)} \frac{\partial I_2(\rho,r)}{\partial r}\bigg|_{r=\rho} \frac{d\rho}{dt} - \frac{p(t)}{\rho} \frac{\partial I_1(\rho,r)}{\partial r}\bigg|_{r=\rho} \frac{d\rho}{dt}$$

$$+ p(t) \frac{I_1(\rho,b)}{\rho I_2(\rho,b)} \frac{\partial I_2(\rho,r)}{\partial r}\bigg|_{r=\rho} \frac{d\rho}{dt} - \frac{bM_o}{\rho I_2(\rho,b)} \frac{\partial I_2(\rho,r)}{\partial r}\bigg|_{r=\rho} \frac{d\rho}{dt}$$

$$- \frac{p(t)}{\rho}\left(\frac{\partial I_1(\rho,r)}{\partial \rho}\bigg|_{r=\rho} - \frac{I_1(\rho,b)}{I_2(\rho,b)} \frac{\partial I_2(\rho,r)}{\partial \rho}\bigg|_{r=\rho}\right)\frac{d\rho}{dt} = 0 \qquad (78)$$

The derivatives that now remain can be evaluated directly, and

$$\frac{\partial I_1(\rho,r)}{\partial r} = \int_\rho^r q(\xi)\xi \, d\xi \qquad \frac{\partial I_1(\rho,r)}{\partial \rho} = -q(\rho)\rho(r - \rho)$$

$$\frac{\partial I_2(\rho,r)}{\partial r} = \frac{b}{2}(r^2 - \rho^2) - \frac{1}{3}(r^3 - \rho^3) \qquad \frac{\partial I_2(\rho,r)}{\partial \rho} = -\rho(r - \rho)(b - \rho) \qquad (79)$$

Since one of these integrals appears in each term of equation (78) and they all become zero as r approaches ρ, the jump condition on moment M_r is identically satisfied.

Initial Hinge Circle Location - Impulsive Loading

Definition of the motion of the hinge circle is the primary difficulty in dynamic plasticity problems. Another basic difficulty is the definition of the initial location of this hinge circle. If the loading

varies from a low value up to a high peak value and then down again, the hinge obviously forms at the origin as $p = p_o$, and moves away from the origin at $p = p_1$. It also reaches a maximum value at some later time and decreases to zero thereafter. This type of smooth motion can be analyzed directly without difficulty. However, if a large step discontinuity in time occurs initially in the loading (as in impulsive loading and other problems), the hinge may form at a location away from the origin. This is the only case in which the hinge may have such a "jump," but this case is important, and location of the initial hinge circle is required. For regime A to exist in the center of the plate, the curvature rates $\dot{\kappa}_r$ and $\dot{\kappa}_\theta$ must be non-negative. Therefore, the initial hinge location ρ_o must be the smaller of the two values that make $\dot{\kappa}_r$ and $\dot{\kappa}_\theta$ non-negative in regime A. Therefore,

$$\dot{\kappa}_r = -\frac{\partial^3 w}{\partial r^2 \partial t} = -\left\{\int \frac{p(t)dt}{\mu}\right\}\frac{\partial^2 q(r)}{\partial r^2} \geq 0$$
$$\dot{\kappa}_\theta = -\frac{1}{r}\frac{\partial^2 w}{\partial r \partial t} = -\frac{1}{r}\left\{\int \frac{p(t)dt}{\mu}\right\}\frac{\partial q(r)}{\partial r} \geq 0 \qquad (80)$$

The only restrictions, then, on initial hinge circle location are that ρ_o must be the smaller of the two values

$$\frac{\partial q(\rho_o)}{\partial \rho_o} \leq 0 \quad \text{and} \quad \frac{\partial^2 q(\rho_o)}{\partial \rho_o^2} \leq 0 \qquad (81)$$

The shape of the loadings is seen to be very important for large initial step loadings.

If the loading is, indeed, a totally impulsive loading, then one additional restriction on ρ_o is possible. For impulsive loading, the load has been applied to the plate instantaneously, and the energy imparted to the plate must be dissipated in plastic deformation as the plate stops. If the hinge circle stayed at ρ_o or increased in size, the energy of plastic deformation would not increase as it should. Therefore, for impulsive loading the hinge circle must decrease or $d\rho/dt$ must be less than zero. For an impulse, $p(t) = 0$, and $\int p(t)dt = \mu V_o$ is the impulse applied to the plate. In this case, then, the initial hinge velocity becomes

$$\left.\frac{d\rho}{dt}\right|_{\rho=\rho_o} = \frac{bM_o}{\mu V_o \rho_2} = \frac{-bM_o\ 12}{\mu V_o(b + 3\rho_o)(\rho_o - b)^2 \left\{\frac{\partial q(\rho_o)}{\partial \rho_o} + \frac{q(\rho_o)}{(b - \rho_o)}\right\}} \tag{82}$$

This velocity is less than zero whenever the following inequality is also true:

$$-\frac{\partial q(\rho_o)}{\partial \rho_o} < \frac{q(\rho_o)}{(b - \rho_o)} \tag{83}$$

Thus, in summary, if a large initial discontinuity in load occurs, the smallest value of ρ_o determined from equations (81) applies. If the loading is truly impulsive at $t = 0$, then the lowest ρ_o from equations (81) or equation (83) must be used. The magnitude of the loading has no effect on these expressions, only the shape of the curve $q(r)$.

Exact Solution - General Impulsive Loadings

For a general impulsive loading, the equation for the motion of the hinge circle can be solved exactly, and since most previous work has been concerned with this type of loading, this general solution is presented here. For the impulsive case $p(t) = 0$ and $\int p(t)dt = \mu V_o$ so that the equation (65) becomes

$$\rho_2 \, d\rho = \frac{bM_o}{\mu V_o} dt \tag{84}$$

and, since the variables are separated, direct integration yields the solution. Using integration by parts, the ρ_2 integral becomes

$$\int \rho_2 \, d\rho = \int I_2(\rho,b) \frac{\partial}{\partial\rho}\left(\frac{q(\rho)}{(\rho - b)}\right) d\rho = \frac{q(\rho)}{(\rho - b)} I_2(\rho,b)$$

$$+ \int \rho q(\rho)(\rho - b)d\rho \tag{85}$$

and after integration of equation (84)

$$\frac{bM_o}{\mu V_o} t + C_4 = - \frac{q(\rho)(b - \rho)^2(b + 3\rho)}{12}\Bigg|_{\rho_o}^{\rho} + \int_{\rho_o}^{\rho} q(\rho)(\rho^2 - b\rho)d\rho \tag{86}$$

Consideration of the initial conditions ($t = 0$, $\rho = \rho_o$) yields $C_4 = 0$. This is the general solution for hinge circle motion. Note that the only integrations that remain are $\int \rho^2 q(\rho)d\rho$ and $\int \rho q(\rho)d\rho$, and these should be directly obtainable for nearly any function. The initial hinge location ρ_o is found to be the smallest value for either equations (81) or equation (83).

Also, the velocity distributions become (from equations (45) and (54))

Regime A
$$\frac{\partial w}{\partial t} = V_o q(r)$$

Regime AB
$$\frac{\partial w}{\partial t} = q(\rho)\,\frac{(r - b)}{(\rho - b)}\,V_o \tag{87}$$

The moment M_r in regime A is M_o, and in regime AB the moment M_r becomes directly from equation (64)

$$M_r = M_o - \frac{12bM_o}{r(b - \rho)^3(b + 3\rho)}\left\{\frac{br}{2}(r^2 - \rho^2) - \frac{(r + b)}{3}(r^3 - \rho^3) + \frac{(r^4 - \rho^4)}{4}\right\} \tag{88}$$

The hinge circle reaches the origin at the time t_1, defined by the left-hand side of equation (86) with $\rho = 0$ on the right-hand side.

$$t_1 = \frac{\mu V_o b^2}{12M_o}\left[-q(o) + q(\rho_o)\left(1 - \frac{\rho_o}{b}\right)^2\left(1 + 3\,\frac{\rho_o}{b}\right) + \frac{12}{b}\int_o^{\rho_o} q(\rho)\,\frac{\rho}{b}\left(1 - \frac{\rho}{b}\right)d\rho\right] \tag{89}$$

After the hinge reaches the origin, $\frac{d\rho}{dt} = 0$ and $\rho = 0$ and since $p(t) = 0$, the acceleration in regime AB vanishes (see eq. (55)), and the velocity distribution in regime AB (eq. (87)) becomes

$$\left.\frac{\partial w}{\partial t}\right|_{t=t_1} = q(o)V_o\left(1 - \frac{r}{b}\right) \tag{90}$$

For values of $t > t_1$, this velocity cannot remain constant in time since energy is still being dissipated. Following the same approach as outlined in reference 5 for a specific $q(r)$, the velocity distribution is assumed to decrease linearly with time ($t > t_1$) until the plate stops.

The velocity distribution then becomes

$$\frac{\partial w}{\partial t} = \frac{\partial w}{\partial t}\bigg|_{t=t_1} + \frac{12M_o}{b^2\mu}(t_1 - t)\left(1 - \frac{r}{b}\right) \qquad (t \geq t_1) \tag{91}$$

The plate finally comes to rest at the time t^* when the velocity drops to zero, so that

$$t^* = t_1 + \frac{\mu V_o q(o) b^2}{12M_o} \tag{92}$$

The solution for M_r in regime AB (eq. (88)) for $\rho = 0$ reduces to

$$M_r = M_o\left(1 - 2\frac{r^2}{b^2} + \frac{r^3}{b^3}\right) \tag{93}$$

Thus, it is noted in this case that the shape of the loading affects only the solution up until the time t_1, and the final conical deflection that decays to zero velocity is the same regardless of the loading shape.

Determination of Final Results

After selection of the loading functions $q(r)$ and $p(t)$, the solution of a general plastic plate problem still remains a complex operation. First of all, the loading must be checked to be certain $p > p_o$ and a hinge will form. Also, $p > p_1$ should be checked to determine if the hinge occurs away from the origin. Assuming it does, the $d\rho/dt$ equation must be solved. The program in the appendix can be used for general cases simply by adding the required definition of the functions in the proper subroutines. After the variation of ρ with time is determined, this value of ρ must be substituted in the proper

expressions for velocity and moment to find their distributions at that particular time. If other quantities are of interest (strains and strain rates, for example), then the velocity expressions (eqs. (45) and (54)) and deflection expressions (such as eqs. (71)) must be integrated or differentiated. In general problems, these manipulations become very difficult if the motion of the hinge circle is more complex than simply an outward then an inward movement. In the simple case of impulsive loading, the exact expressions can be written in a straightforward manner.

Example Cases

To illustrate the influence of the time variation of loading, several example cases were computed for general loading functions. To allow a general type of loading that may be expected in practice, the loading $q(r)$ was selected to be Gaussian, and the time variation of the load was considered to be essentially exponentially decaying. Since the combination of general radial and time functions has not been attempted before, some latitude exists as to the exact shapes to select. For the examples herein, then, the radial distribution is

$$q(r) = e^{-a^2r^2} = e^{-r^2} \tag{94}$$

This load decreases from a maximum at the origin to approximately 38 percent of its maximum value at the support ($r = b = 1$), and is non-uniform. The time function was selected so that a uniform load was applied until a small total impulse had been given to the plate, then an exponential decay was assumed. The general shape considered is shown in figure 7. The loading remained constant until an impulse of 1×10^{-4} had been

applied. Thereafter, the loading dropped of exponentially as $e^{-\alpha t}$, and the value of α decided how rapidly the loading decreased. The total impulse applied to the plate during the unloading phase was also held constant at one. Attention is centered on solution for the hinge circle movement, since this motion is considered the basic kernel of the problem.

The first sample case is shown for $\alpha = 1$ in figure 8. Since these cases all have an initial jump in loading, the hinge starts at a location other than the origin. In this case, the hinge starts at $\rho_o = \sqrt{2}/2$ (as required by the radial load distribution), but it quickly moves to the origin of the plate. This same type of motion has been seen previously for uniform loading and is an example of a continually decreasing hinge circle.

The second sample case is shown for $\alpha = 1 \times 10^5$ in figure 9. In this case, the first example of an outward moving hinge circle is seen. Due to the radial load distribution again, this hinge also starts at $\rho_o = \sqrt{2}/2$, but soon after the load variation starts, the hinge moves out to a maximum value of 0.984 before it slowly moves inward. Note that the hinge circle moved outward even though the loading is decreasing with time. Previous results on very high impulsive loadings (ref. 2) indicate that the initial hinge circle location was seen to approach b only as the loading approached infinity. Therefore, this example of a high initial loading seems to verify this effect. Note also that even after the same total impulse has been applied in both cases, the location of the hinge circle is vastly different from case 1 due to the time factor only. Perzyna (ref. 37), for a uniform radial distribution and different time expressions, states that the influence of time variation of the loading

is unimportant in determination of hinge circle location, but this is not generally the case. The velocity and moment distributions have been calculated for case 1 and are shown in figures 10 and 11, respectively. As expected, figure 10 shows the velocity distribution is linear (or conical) in the region outside of the hinge circle. The shape of the velocity distribution inside of the hinge circle is non-uniform and of the same general shape as the loading function $q(r)$. However, it can be seen that the velocity in the central region of the plate is continually increasing. This effect was not seen previously (ref. 36) for impulsive loading of this general shape, and is caused by the time variation of the loading. The moment distributions in figure 11 are seen to smoothly decay from M_o at the hinge circle to zero at the support. There appears to be no discontinuity in slope at the hinge, and the curves tend to have a slight reverse curvature near the support (especially for later times).

The velocity and moment distributions have also been calculated for case 2, and are shown in figures 12 and 13, respectively. Since the hinge circle has been allowed to move outward, the velocity distributions in the center region of the plate have a reverse curvature in them at $r = 0.707\ b$. This same reverse curvature exists in $q(r)$, and the shapes of the velocity distributions agree with $q(r)$ out to the hinge circle. These distributions are also conical in the outer region of the plate. The increase of velocity with time in the central region is even more pronounced in this case than in case 1. The moment distributions in the

plate for case 2 (fig. 13) show that for early times the moment distribution is similar in form to case 1. However, as the hinge moves outward with time, the moment distribution becomes steeper and the reverse curvature seen only slightly in figure 11 becomes very pronounced in this case.

CONCLUSIONS

From the results and equations shown herein, several important conclusions are evident. The equations derived here considering bending deformations only are seen to be more general in form than existing solutions, and reduction to the existing cases is direct. For example if the loading is considered uniform in r and impulsive or step-wise uniform in time, the equations derived directly for such cases by Hopkins and Prager and Wang (refs. 2 and 5) appear exactly. Also, if the radial load distribution is considered uniform, and a general function of time is allowed (but assuming only inward hinge circle movement), the non-linear equations of Perzyna (ref. 37) are found exactly. The conclusion of Perzyna that time variation is unimportant appears to be caused by an unfortunate choice of example time functions. He solves the specific non-linear equations for his example, and does not present any means for evaluation of his numerical method of solution.

If the loading on the plate is considered to be a distributed Gaussian loading in r and impulsively applied, the equations derived directly for this case by Thomson (ref. 36) appear exactly herein. These two papers (by Perzyna and Thomson) are the only two papers available at present that allow variations of the loading, one in r and the other in t, and both sets of equations are included in the general expressions herein. In fact, the solutions currently available for bending theory are found to exist as special cases of these general equations.

Two other results presented herein are also of direct interest. The equations for impulsive loading of general radial shape are shown to be directly solvable, and expressions for the solution are written. Many cases of practical interest are, therefore, seen to be available now in a direct manner without numerical integration or other approximation. Also, the general load-carrying capacity of circular plates under arbitrary radial load distribution is presented for the Tresca yield criterion. This load value (p_o) is known to yield a lower (conservative) bound for the load-carrying capacity and can be used effectively for design purposes.

REFERENCES

1. Hopkins, H. G.; and Prager, W.: The Load Carrying Capacities of Circular Plates. J. Mech. Phys. Solids, vol. 2, no. 1, October 1953, pp. 1-13.

2. Hopkins, H. G.; and Prager, W.: On the Dynamics of Plastic Circular Plates. Z.A.M.P., vol. 5, 1954, pp. 317-330.

3. Prager, W.: The General Theory of Limit Design. Proceedings of the 8th Int. Con. Appl. Mech. (Istanbul, 1952), vol. 2, pp. 65-72.

4. Hopkins, H. G.; and Wang, A. J.: Load-Carrying Capacities for Circular Plates of Perfectly-Plastic Material with Arbitrary Yield Condition. J. Mech. Phys. Solids, vol. 3, 1955, pp. 117-129.

5. Wang, A. J.: The Permanent Deflection of a Plastic Plate Under Blast Loading. J. Appl. Mech., vol. 22, 1955, pp. 375-376.

6. Wang, A. J.; and Hopkins, H. G.: On the Plastic Deformation of Built-In Circular Plates Under Impulsive Load. J. Mech. Phys. Solids, vol. 3, no. 1, October 1954, pp. 22-37.

7. Wierzbicki, T.: Bending of a Rigid, Visco-plastic Circular Plate. Arch. Mech. Stos., vol. 16, no. 6, 1964, pp. 1183-1195.

8. Frederick, D.: A Simplified Analysis of Circular Membranes Subjected to an Impulsive Loading Producing Large Plastic Deformations. 4th Midwest Conf. Solid Mech., Univ. of Texas, 1959, pp. 18-35.

9. Murakami, S.; and Ookhasi, I.: Uniaxial Elasto-plastic Bending of a Circular Plate with Radial Tension, Inz. Shurnal, vol. 5, no. 1, 1965.

10. Jones, N.: Impulsive Loading of a Simply-Supported Circular Rigid Plastic Plate, J. Appl. Mech., March 1968, pp. 59-65.

11. Sawczuk, A.: On Initiation of the Membrane Action in Rigid-Plastic Plates, J. de Mecanique, vol. 3, no. 1, March 1964, pp. 15-23.

12. Onat, E. T.; and Haythornthwaite, R. M.: The Load-Carrying Capacity of Circular Plates at Large Deflection. J. Appl. Mech., vol. 23, 1956, pp. 49-55.

13. Kruszewski, E. T.: Influence of Large Deformation and Mid-Plane Forces on the Plastic Behavior of Impulsively Loaded Plates. Ph. D. Thesis, V.P.I., 1968.

14. Onat, E. T.; and Prager, W.: Limit Analysis of Shells of Revolution. Proc. Royal Netherlands Acad. of Sci. Parts I and II, series B, vol. 57, 1954, pp. 534-548.

15. Kochetkov, A. M.: On the Propagation of Elastic-Visco-Plastic Shear Waves in Plates. P.M.M., vol. 14, no. 2, 1950, pp. 203-208.

16. Kojasteh-Bakht, M.; Yaghmai, S; and Popov, E. P.: A Bending Analysis of Elastic-Plastic Circular Plates. Calif. U., Struc. Engr. Lab., April 1966, SESM 66-4.

17. Dong, S. B.; and Hilton, H. H.: An Analogy for Anisotropic, Non-homogeneous, Linear Viscoelasticity Including Thermal Stresses. Proceedings the 8th Midwest Mech. Conf. (Case Inst., Cleveland, Ohio, 1963), vol. 2, pt. 2, pp. 58-73.

18. Salvadori, M. G.; and Weidlinger, P.: On the Dynamic Strength of Rigid Plastic Beams Under Blast Loads. Proc. ASCE vol. 83, no. EM 4, paper 1389, October 1957.

19. Sankaranarayanan, R.: On the Dynamics of Plastic Spherical Shells. J. Appl. Mech., vol. 30, no. 1, 1963, pp. 87-90.

20. Symonds, P. S.: Plastic Shear Deformations in Dynamic Load Problems. Div. of Engr., Brown U. Rpt. NSK-GK1013X/4, April 1967.

21. Huszek, M.; and Sawczuk, A.: A Note on the Interaction of Shear and Bending in Plastic Plates. Arch. Mech. Stos., vol. 15, no. 3, 1968, pp. 411-426.

22. Thomson, R. G.: Analysis of Hypervelocity Perforation of a Visco-Plastic Solid Including the Effects of Target-Material Yield Strength. NASA TR R-221, April 1965.

23. Mentel, T. J.; and Schultz, R. L.: Visco-Elastic Support Damping of Built-In Circular Plates. Wright-Pat. A.F.B., ASD-TDR-63-648, October 1963.

24. Sundstroem, E.: Membrane Creep and Plastic Deformations of Annular Plates. Ark. foer Fyz., vol. 29, no. 5, 1965, pp. 403-422.

25. Florence, A. L.: Clamped Circular Rigid-Plastic Plates Under Blast Loading. A.S.M.E. Western Conf., L. A., Calif., 1965, paper 65, APMW 34.

26. French, F. W.: Elastic-Plastic Analysis of Centrally-Clamped Annular Plates Under Uniform Loads. Mitre Corp. Rept. AF-ESD-TDR-63-398, December 1962.

27. Florence, A. L.: Annular Plate Under a Transverse Line Impulse. AIAA Journ., vol. 3, September 1965, pp. 1726-1732.

28. Kececioglu, D.: Bibliography on Plasticity-Theory and Application. A.S.M.E. publication, 1950.

29. Goodier, J. N.; and Hodge, P. G., Jr.: Elasticity-Plasticity. Wiley, New York, 1958.

30. Olszak, W.; Mroz, Z.; and Perzyna, P.: Recent Trends in the Development of the Theory of Plasticity. MacMillan (Pergamon), 1963.

31. Kachanov, L. M.: Investigations of Elasticity and Plasticity, Leningrad, Izv. Leningrad U., 1964 (in Russian).

32. Solid Mechanics Seminar, Lecture Abstracts, held at Brown Univ. June 8-17, 1967.

33. Florence, A. L.; and Firth, R. D.: Rigid-Plastic Beams under Uniformly Distributed Impulses. Trans. of the A.S.M.E., paper no. 65, APM, J. Appl. Mech., 1965.

34. Munday, G.; and Newitt, D. M.: The Deformation of Transversely-Loaded Disks under Dynamic Loads. Phil. Trans. Royal Soc., Series A, no. 1065, vol. 256, December 1963, pp. 1-30.

35. Florence, A. L.: Circular Plate Under a Uniformly Distributed Impulse. Int. J. of Solids and Struc., vol. 2, January 1966, pp. 37-47.

36. Thomson, R. G.: Plastic Deformation of Plates Subjected to a General Gaussian Distribution of Impulse. Ph. D. Thesis, V.P.I., 1966.

37. Perzyna, P.: Dynamic Load Carrying Capacity of a Circular Plate. Arch. Mech. Stos., vol. 10, 1958, pp. 635-647.

38. Sankaranarayanan, R.: On the Impact Pressure Loading of a Plastic Spherical Cap. J. Appl. Mech., vol. 33, no. 3, September 1966, pp. 704-706.

39. Goldsmith, W.; Liu, T. W.; and Chulay, S.: Plate Impact and Perforation by Projectiles. Exp. Mech. Journ. (S.E.S.A.), December 1965, pp. 385-404.

40. Haythornthwaite, R. M.: The Range of the Yield Condition in Stable, Ideally Plastic Solids. Proc. A.S.C.E., vol. 87, J. of Engr. Mech. Div., December 1961, pp. 117-133.

41. Masket, A. V.: The Measurement of Forces Resisting Armor Penetration. J. Appl. Phys., vol. 20, 1949, p. 132.

42. Karas, K.: Platten unter seitlichem Stoss. Ingr.-Arch., vol. 10, 1939, p. 237.

The vita has been removed from the scanned document

APPENDIX

GENERAL COMPUTER PROGRAM FOR HINGE CIRCLE MOTION

A general computer program that solves the $d\rho/dt$ equation (eq. (65)) for arbitrary functions of r and t has been written in Fortran IV computer language, and a listing of the deck is included in this appendix. Many comment cards have been included in the deck to directly define the expressions and quantities involved and should be essentially self-explanatory. If a new radial distribution is to be investigated, it must be defined in the function $Q(R)$, and its first and second derivatives written as the functions $QP(R)$ and $QPP(R)$, respectively. If the exact expression for $I_1(\rho,b)$ can be written, this expression should be put into the subroutine IlEX. If it cannot be expressly written, the main program will numerically integrate (simply set $IEX = 0$). Similarly, if a new time function is to be investigated, it must be defined in the function $P(T)$. If the exact expression for $\int p(t)dt$ can be written, this expression should also be included in the subroutine PTEX. If not, the main program will integrate numerically (simply set $NEX = 0$). A sample case is also included, and the initial printout shows the procedure used in the machine to determine the initial hinge circle location. If a totally impulsive loading is applied to the plate, an additional possible restriction on ρ_0 (eq. (83)) must also be considered. However, for impulsive loading it is more reasonable to use the exact expressions derivable as shown in the text.

```
      PROGRAM GENPLAS (INPUT,OUTPUT)
C     THIS IS THE MAIN PROGRAM FOR SOLUTION OF THE DRHO/DT EQUATION
C     AND IS THE SAME FOR ALL GENERAL TYPES OF LOADINGS
C     B=RADIUS OF THE PLATE ,MZ=INITIAL YIELD MOMENT  M ZERO
C     I1, I2, RHO1, RHO2 ARE DEFINED FUNCTIONS OF THE HINGE LOCATION
C     TZ=INITIAL TIME, A SHORT TIME DURING WHICH THE LOAD IS CONSTANT
C     DELT IS AN EXPECTED TIME STEP USED TO PLOT RHO VS TIME
C     E1,E2, ARE RELATIVE ERRORS USED IN ITR2 TO FIND RHO INITIAL
C     MAXI= MAXIMUM NUMBER OF STEPS ALLOWED IN RHO VS TIME RESULTS
C     RB,RE,RI ARE THE STARTING ,ENDING ,AND INCREMENT VALUES OF RHOZ
C                                        USED IN THE ITR2 ROUTINE
C     K1,K2,K3,K4 ARE INTERMEDIATE ANS. USED IN THE RUNG-KUTTA SOL.
C     A IS A CONSTANT THAT TYPIFIES THE RADIAL LOAD VARIATION
C     ALPHA IS A CONSTANT THAT TYPIFIES THE TIME LOAD VARIATION
C     IEX=0 USE NUMERICAL INTEGR. FOR I1,IEX=NON-0 EXACT EXPR. IS USED
C     NEX=0 USE NUMERICAL INTEGR. FOR PT,NEX=NON-0 EXACT EXPR. IS USED
C     DERSUB IS THE ROUTINE THAT CALCULATES DERIVATIVE DRHO/DT
C     RHOINT IS THE ROUTINE THAT CALCULATES THE INITIAL HINGE LOCATION
C     ANS ALWAYS REFERS TO THE DERIVATIVE DRHO/DT
C     X AND Y REFER TO TIME AND RHO IN RUNG-KUTTA SOLUTION
C     ITR2 IS A MACHINE ROUTINE THAT SOLVES FOR THE ZEROS OF A FUNCTION
C     MGAUSS IS A MACHINE ROUTINE THAT INTEGRATES NUMERICALLY
      DIMENSION RESULT(2)
      REAL K1,K2,K3,K4,MZ,I1,I2
      COMMON/BLK1/B,A,ALPHA
      COMMON/BLK2/MZ
      COMMON/BLK3/I1,I2,RHO1,RHO2
      COMMON/BLK4/E1,E2,MAXI,TZ
      COMMON/BLK5/IEX,NEX
      COMMON/BLK6/IRR
      NAMELIST/INPUT/TZ,MZ,B,A,DELT,ALPHA,MAXI,E1,E2,IEX,NEX
    1 CALL DAYTIM (RESULT)
      PRINT 2, RESULT
    2 FORMAT(*1DATE*3XA10,5X*TIME*3XA10/* ROBINSON-WEIDMAN, SRD-A2058, R
     1DP-308*/* GENERAL PRESSURE LOADING ON PLASTIC THIN PLATES*//)
      READ INPUT
      IF (IEX.EQ.0)   PRINT  25
      IF (NEX.EQ.0)   PRINT 30
   25 FORMAT( *ONUMERICAL INTEGR. USED FOR I1*)
   30 FORMAT( *ONUMERICAL INTEGR. USED FOR PT*)
    3 CALL RHOINT(RHOZ)
      PRINT 20, MZ,ALPHA,B,A,DELT,RHOZ,TZ
```

```
20 FORMAT(5X*MZ=*E15.8,5X*ALPHA=*E15.8/
  16X*B=*E15.8,9X*A=*E15.8/
  23X*DELT=*E15.8,6X*RHOZ=*E15.8/
  35X*TZ=*E15.8//)
   PRINT 4
 4 FORMAT(10X*T*,16X*RHO*,16X*I1*,16X*I2*,15X*RHO1*,14X*RHO2*,14X*ANS
  1*//)
   RHO=RHOZ
   T=TZ
   H=DELT
   I=0
 5 X=T
   Y=RHO
   CALL DERSUB (X,Y,ANS)
   PRINT 8, X,Y,I1,I2,RHO1,RHO2,ANS
 8 FORMAT(7(3XE15.8))
   IF (RHO.LE.0.0) GO TO 1
   K1=ANS*H
   X=T+H/2.
   Y=RHO+K1/2.
   CALL DERSUB (X,Y,ANS)
   K2=ANS*H
   Y=RHO+K2/2.
   CALL DERSUB (X,Y,ANS)
   K3=ANS*H
   X=T+H
   Y=RHO+K3
   CALL DERSUB (X,Y,ANS)
   K4=ANS*H
   DELRHO=(K1+2.*K2+2.*K3+K4)/6.
   I=I+1
   IF (I.GT.MAXI) GO TO 6
   IF(ABS(DELRHO).GE..15*B)  GO TO 9
   IF(ABS(DELRHO).LE..001*B.AND.ABS(ANS).GE.1.E+2)  GO TO 10
   T=T+H
   RHO=RHO+DELRHO
   GO TO 5
 6 PRINT 7
 7 FORMAT(5X*MAXIMUM NUMBER OF STEPS TAKEN*//)
   GO TO 1
 9 DELT=DELT*.2
12 PRINT 15,DELT
15 FORMAT(5X*DELT HAS BEEN CHANGED TO *E15.8)
```

```
      H=DELT
      GO TO 5
   10 DELT=DELT*5.
      H=DELT
      PRINT 15,DELT
      GO TO 5
      STOP
      END
```

```
      SUBROUTINE DERSUB (T,RHO,ANS)
C     THIS ROUTINE CALCULATES THE DERIVATIVE DRHO/DT
C     AND IS THE SAME FOR ALL GENERAL TYPES OF LOADINGS
C     FUNC1,FUNC2,FOFX1,FOFX2,SUM1,SUM2 ARE ALL ADDED FOR INTEGR. ROUT.
C     I1EX CONTAINS THE EXACT EXPR. FOR I1 IF ANALYTICALLY KNOWN
C     PTEX CONTAINS THE EXACT EXPR. FOR PT IF ANALYTICALLY KNOWN
C     FOR OTHER DEFINITIONS OF FUNCTIONS SEE MAIN PROGRAM
      EXTERNAL FUNC1,FUNC2
      DIMENSION SUM1(1),FOFX1(1),SUM2(1),FOFX2(1)
      REAL I2,I1,MZ,NUM,I2A
      COMMON/BLK1/B,A,ALPHA
      COMMON/BLK2/MZ
      COMMON/BLK3/I1,I2,RHO1,RHO2
      COMMON/BLK5/IEX,NEX
      I2=-(RHO-B)**3*(3.*RHO+B)/12.
      I2A=(B-RHO)*(3.*RHO+B)/12.
      IF (IEX.EQ.0) GO TO 1
      CALL I1EX (I1,RHO)
      GO TO 2
    1 INT=(B-RHO)*10.
      CALL MGAUSS (RHO,B,INT,SUM1,FUNC1,FOFX1,1)
      I1=SUM1(1)
    2 RHO2=I2A*(QP(RHO)*(RHO-B)-Q(RHO))
      RHO1=I1+Q(RHO)*I2A*(RHO-B)
      IF (NEX.EQ.0) GO TO 3
      CALL PTEX (PT,T)
      GO TO 4
    3 CALL MGAUSS (0.,T,30,SUM2,FUNC2,FOFX2,1)
      PT=SUM2(1)
    4 DEN=PT*RHO2
      NUM=B*MZ-P(T)*RHO1
      ANS=NUM/DEN
      RETURN
      END
```

```
      SUBROUTINE  RHOINT (RHOZ)
C     THIS ROUTINE CALCULATES THE INITIAL HINGE LOCATION
C     AND IS THE SAME FOR ALL GENERAL TYPES OF LOADINGS
C     ICODE IS AN ERROR DIAGNOSTIC WRITTEN TO DEFINE WHERE THE MIN.
C     VALUE FOUND BY ITR2 IS LOCATED.
C     ICODE=0 PROPER RETURN... ICODE=3 THEN RHO OUTSIDE OF THE PLATE
C     ROIN IS ANOTHER EXPR. WRITTEN FOR RHO INITIAL.
C     FOR OTHER DEFINITIONS OF FUNCTIONS SEE MAIN PROGRAM
      COMMON/BLK1/B,A,ALPHA
      COMMON/BLK4/E1,E2,MAXI,TZ
      COMMON/BLK6/IRR
      EXTERNAL QPP
      EXTERNAL  QP
      RB=.001*B
      RE=1.0*B
      RI=.1*B
      CALL ITR2 (RHOZ,RB,RE,RI,QPP,E1,E2,MAXI,ICODE)
      IF (ICODE.NE.0) PRINT 1, ICODE
      PRINT  2
    2 FORMAT(*0*//)
      IRR=0
    1 FORMAT(*0ERROR FROM ITR2- QPP---ICODE=*I3/)
      IF( ICODE.EQ.3) RHOZ=0.
      IF(ICODE.EQ.3.AND.QPP(0.).LE.0.)  RHOZ=B
      PRINT  2
      RC=.001*B
      CALL ITR2 (ROIN,RC,RE,RI,QP ,E1,E2,MAXI,ICODE)
      IF (ICODE.NE.0) PRINT 3, ICODE
      PRINT  2
    3 FORMAT(*0ERROR FROM ITR2- QP ---ICODE=*I3/)
      IF( ICODE.EQ.3) ROIN=0.
      IF(ICODE.EQ.3.AND.QP (0.).LE.0.)  ROIN=B
      PRINT  2
      IRR=1
      IF(ROIN.LE.RHOZ)  RHOZ=ROIN
      RETURN
      END
```

```
      SUBROUTINE FUNC1 (X,FOFX1)
C     THIS ROUTINE IS SIMPLY AN INTEGR. NECESSITY
C     AND IS THE SAME FOR ALL GENERAL TYPES OF LOADINGS
      DIMENSION FOFX1(1)
      COMMON/BLK1/B,A,ALPHA
      FOFX1(1)=(B-X)*Q(X)*X
      RETURN
      END
```

```
      SUBROUTINE FUNC2 (X,FOFX2)
C     THIS ROUTINE IS SIMPLY AN INTEGR. NECESSITY
C     AND IS THE SAME FOR ALL GENERAL TYPES OF LOADINGS
      DIMENSION FOFX2(1)
      FOFX2(1)=P(X)
      RETURN
      END
```

```
      FUNCTION Q(R)
C     THIS ROUTINE IS WHERE THE RADIAL DISTRIBUTION IS DEFINED
C     AND MUST BE INDIVIDUALLY WRITTEN FOR EACH LOADING SHAPE...
      COMMON/BLK1/B,A,ALPHA
      Q=EXP(-A**2*R*R)
      RETURN
      END
```

```
      FUNCTION QP(R)
C     THIS ROUTINE CALCULATES THE FIRST  DERIVATIVE OF THE RADIAL LOAD
C     DISTRIBUTION AND MUST BE WRITTEN FOR EACH LOADING SHAPE...
      COMMON/BLK1/B,A,ALPHA
      COMMON/BLK6/IRR
      QP=-2.*A*A*R*EXP(-A**2*R**2)
      IF (IRR.EQ.0) PRINT 1,R,QP
    1 FORMAT(5X*RHO=*E15.8,5X*QP=*E15.8)
      RETURN
      END
```

```
      FUNCTION QPP(RHO)
C     THIS ROUTINE CALCULATES THE SECOND DERIVATIVE OF THE RADIAL LOAD
C     DISTRIBUTION AND MUST BE WRITTEN FOR EACH LOADING SHAPE...
      COMMON/BLK1/B,A,ALPHA
      QPP=EXP(-A**2*RHO**2)*(-2.*A**2+4.*A**4*RHO**2)
      PRINT 1, RHO,QPP
    1 FORMAT(5X*RHO=*E15.8,5X*QPP=*E15.8)
      RETURN
      END
```

```
      FUNCTION P(T)
C     THIS ROUTINE IS WHERE THE  TIME DISTRIBUTION IS DEFINED
C     AND MUST BE INDIVIDUALLY WRITTEN FOR EACH TIME VARIATION....
      COMMON/BLK1/B,A,ALPHA
      CONST=.1E-3/ALPHA
      IF (T.LE.CONST) GO TO 1
      P=ALPHA*EXP(-ALPHA*(T-CONST))
      RETURN
    1 P=ALPHA
      RETURN
      END
```

```
      SUBROUTINE I1EX (I1,RHO)
C     THIS ROUTINE CALCULATES EXACT EXPR. FOR I1 IF ANALYTICALLY KNOWN
C     AND MAY BE WRITTEN OR OMITTED FOR EACH SPECIFIC RADIAL LOADING
C     TYPIFIED BY A PARAMETER A
C     SET IEX=NON-0  ON $INPUT CARD TO USE THIS ROUTINE
      REAL I1
      COMMON/BLK1/B,A,ALPHA
      PI=3.14159265358979
      I1=(EXP(-A**2*RHO**2)*(A*B-A*RHO)/2.+SQRT(PI)*(ERF(A*RHO)-
     1ERF(A*B))/4.)/A**3
      RETURN
      END
```

```
      SUBROUTINE PTEX (PT,T)
C     THIS ROUTINE CALCULATES EXACT EXPR. FOR PT IF ANALYTICALLY KNOWN
C     AND MAY BE WRITTEN OR OMITTED FOR EACH SPECIFIC RADIAL LOADING
C     TYPIFIED BY A PARAMETER ALPHA
C     SET NEX=NON-0  ON $INPUT CARD TO USE THIS ROUTINE
      COMMON/BLK1/B,A,ALPHA
      X=ALPHA*T
      IF (X.GT.1.E-4) GO TO 1
      PT=X
      RETURN
    1 PT=1.0+1.E-4-EXP(-(X-1.E-4))
      RETURN
      END
```

```
DATE    04/23/68       TIME    13.26.25.
ROBINSON-WEIDMAN, SRD-A2058, RDP-308
GENERAL PRESSURE LOADING ON PLASTIC THIN PLATES

     RHO= 1.00000000E-03      QPP=-1.99999400E+00
     RHO= 1.01000000E-01      QPP=-1.93931183E+00
     RHO= 2.01000000E-01      QPP=-1.76560331E+00
     RHO= 3.01000000E-01      QPP=-1.49575084E+00
     RHO= 4.01000000E-01      QPP=-1.15525955E+00
     RHO= 5.01000000E-01      QPP=-7.74906395E-01
     RHO= 6.01000000E-01      QPP=-3.86882181E-01
     RHO= 7.01000000E-01      QPP=-2.10423964E-02
     RHO= 8.01000000E-01      QPP= 2.98182765E-01
     RHO= 7.51000000E-01      QPP= 1.45647901E-01
     RHO= 7.26000000E-01      QPP= 6.39349454E-02
     RHO= 7.13500000E-01      QPP= 2.18354342E-02
     RHO= 7.07250000E-01      QPP= 4.91341929E-04
     RHO= 7.04125000E-01      QPP=-1.02521363E-02
     RHO= 7.05687500E-01      QPP=-4.87450984E-03
     RHO= 7.06468750E-01      QPP=-2.19010718E-03
     RHO= 7.06859375E-01      QPP=-8.49012818E-04
     RHO= 7.07054687E-01      QPP=-1.78742915E-04
     RHO= 7.07152344E-01      QPP= 1.56322649E-04
     RHO= 7.07103516E-01      QPP=-1.12043490E-05
     RHO= 7.07127930E-01      QPP= 7.25605961E-05
     RHO= 7.07115723E-01      QPP= 3.06784851E-05
     RHO= 7.07109619E-01      QPP= 9.73715841E-06



     RHO= 0.                  QPP=-2.00000000E+00



     RHO= 1.00000000E-03      QP=-1.99999800E-03
     RHO= 1.01000000E-01      QP=-1.99949872E-01
     RHO= 2.01000000E-01      QP=-3.86082504E-01
     RHO= 3.01000000E-01      QP=-5.49856011E-01
     RHO= 4.01000000E-01      QP=-6.82872119E-01
     RHO= 5.01000000E-01      QP=-7.79577637E-01
     RHO= 6.01000000E-01      QP=-8.37600382E-01
     RHO= 7.01000000E-01      QP=-8.57699725E-01
     RHO= 8.01000000E-01      QP=-8.43371145E-01
     RHO= 9.01000000E-01      QP=-8.00191791E-01
     RHO= 1.00000000E+00      QP=-7.35758882E-01

ERROR FROM ITR2- QP ---ICODE=  3
```

RHO= 0. QP= 0.

MZ= 1.00000000E+00 ALPHA= 1.00000000E+00
B= 1.00000000E+00 A= 1.00000000E+00
DELT= 1.00000000E-06 RHOZ= 7.07109619E-01
TZ= 1.00000000E-04

T	RHO	I1	I2	RHO1	RHO2	ANS
1.00000000E-04	7.07109619E-01	1.79208405E-02	6.53542158E-03	4.38704800E-03	-2.70679560E-02	-3.67819776E+05
DELT HAS BEEN CHANGED TO 2.00000000E-07						
1.00000000E-04	7.07109619E-01	1.79208405E-02	6.53542158E-03	4.38704800E-03	-2.70679560E-02	-3.67819776E+05
1.00200000E-04	6.39193809E-01	2.74097391E-02	1.14199364E-02	6.37434955E-03	-3.14096955E-02	-3.15712187E+05
1.00400000E-04	5.79702511E-01	3.71671025E-02	1.69472104E-02	8.35369678E-03	-3.51483818E-02	-2.81007396E+05
1.00600000E-04	5.26272433E-01	4.68857628E-02	2.28467959E-02	1.03251654E-02	-3.86947503E-02	-2.54239193E+05
1.00800000E-04	4.77706542E-01	5.63142625E-02	2.88885653E-02	1.22888079E-02	-4.22300685E-02	-2.32031882E+05
1.01000000E-04	4.33247645E-01	6.52676865E-02	3.48881586E-02	1.42446724E-02	-4.58157983E-02	-2.13025949E+05
1.01200000E-04	3.92324926E-01	7.36257829E-02	4.07086237E-02	1.61928058E-02	-4.94487266E-02	-1.96595866E+05
1.01400000E-04	3.54462046E-01	8.13273660E-02	4.62556307E-02	1.81332541E-02	-5.30938919E-02	-1.82376993E+05
1.01600000E-04	3.19245147E-01	8.83458340E-02	5.14689129E-02	2.00660628E-02	-5.67041161E-02	-1.70093816E+05
1.01800000E-04	2.86311524E-01	9.46853906E-02	5.63130329E-02	2.19912770E-02	-6.02306001E-02	-1.59506279E+05
1.02000000E-04	2.55344052E-01	1.00365093E-01	6.07693162E-02	2.39089414E-02	-6.36278755E-02	-1.50398246E+05
1.02200000E-04	2.26066446E-01	1.05412046E-01	6.48295976E-02	2.58191003E-02	-6.68555035E-02	-1.42577694E+05
1.02400000E-04	1.98238294E-01	1.09856244E-01	6.84916659E-02	2.77217976E-02	-6.98780808E-02	-1.35878163E+05
1.02600000E-04	1.71649886E-01	1.13727325E-01	7.17560898E-02	2.96170770E-02	-7.26646608E-02	-1.30158872E+05
1.02800000E-04	1.46117194E-01	1.17052627E-01	7.46240156E-02	3.15049818E-02	-7.51866711E-02	-1.25303579E+05
1.03000000E-04	1.21477132E-01	1.19856031E-01	7.70956137E-02	3.33855550E-02	-7.74187493E-02	-1.21218797E+05
1.03200000E-04	9.75831865E-02	1.22157273E-01	7.91689140E-02	3.52588391E-02	-7.93355770E-02	-1.17831986E+05
1.03400000E-04	7.43016810E-02	1.23971471E-01	8.08388297E-02	3.71248765E-02	-8.09117098E-02	-1.15090143E+05
1.03600000E-04	5.15064499E-02	1.25308709E-01	8.20962115E-02	3.89837091E-02	-8.21201549E-02	-1.12959126E+05
1.03800000E-04	2.90780475E-02	1.26173537E-01	8.29267791E-02	4.08353787E-02	-8.29310087E-02	-1.11424053E+05
1.04000000E-04	6.89673601E-03	1.26564261E-01	8.33097690E-02	4.26799265E-02	-8.33098241E-02	-1.10491207E+05
1.04200000E-04	-1.51606201E-02	1.26471863E-01	8.32160749E-02	4.45173935E-02	-8.32155058E-02	-1.10192220E+05

TABLE 1.- POSSIBLE PLASTICITY REGIMES FOR CIRCULAR PLATES WITH VARIOUS YIELD CONDITIONS

Yield conditions	Possible regimes	
	Simply supported	Clamped
von Mises	AC	AE
Tresca	A, AB	A, AB, BD, D
Johansen	A, AB	A, AC, C, CD
Haythornthwaite	AB, BC	AB, BD, DE

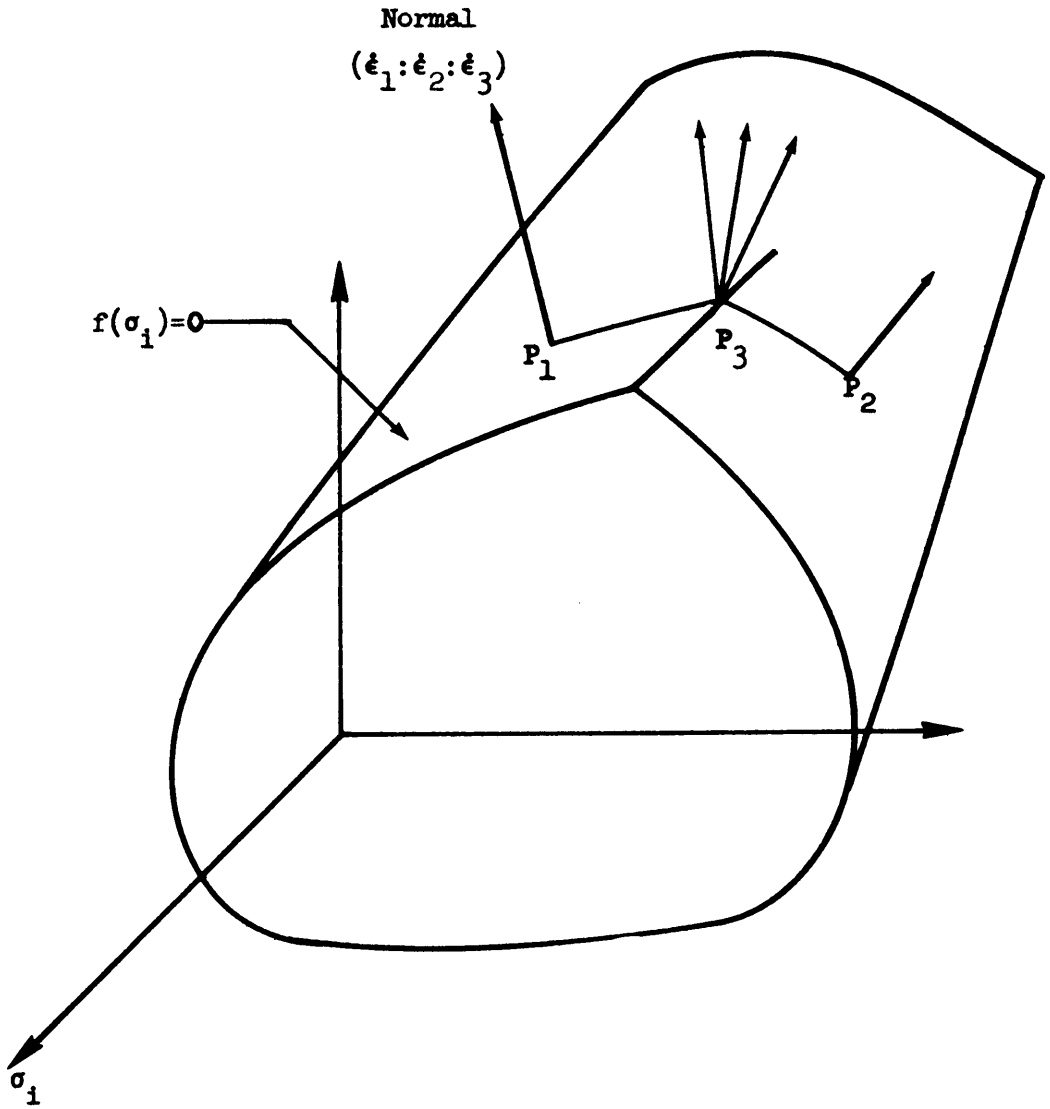

Figure 1. – Generalized yield conditions and flow rules.

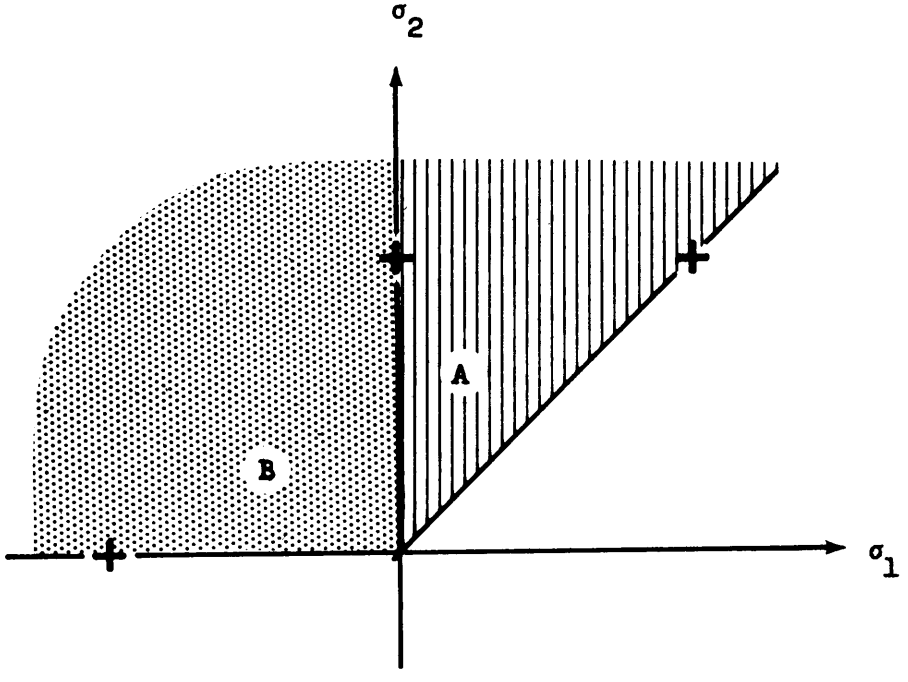

Figure 2. – Yield regions determined by boundary conditions in plane stress problems for circular plates.

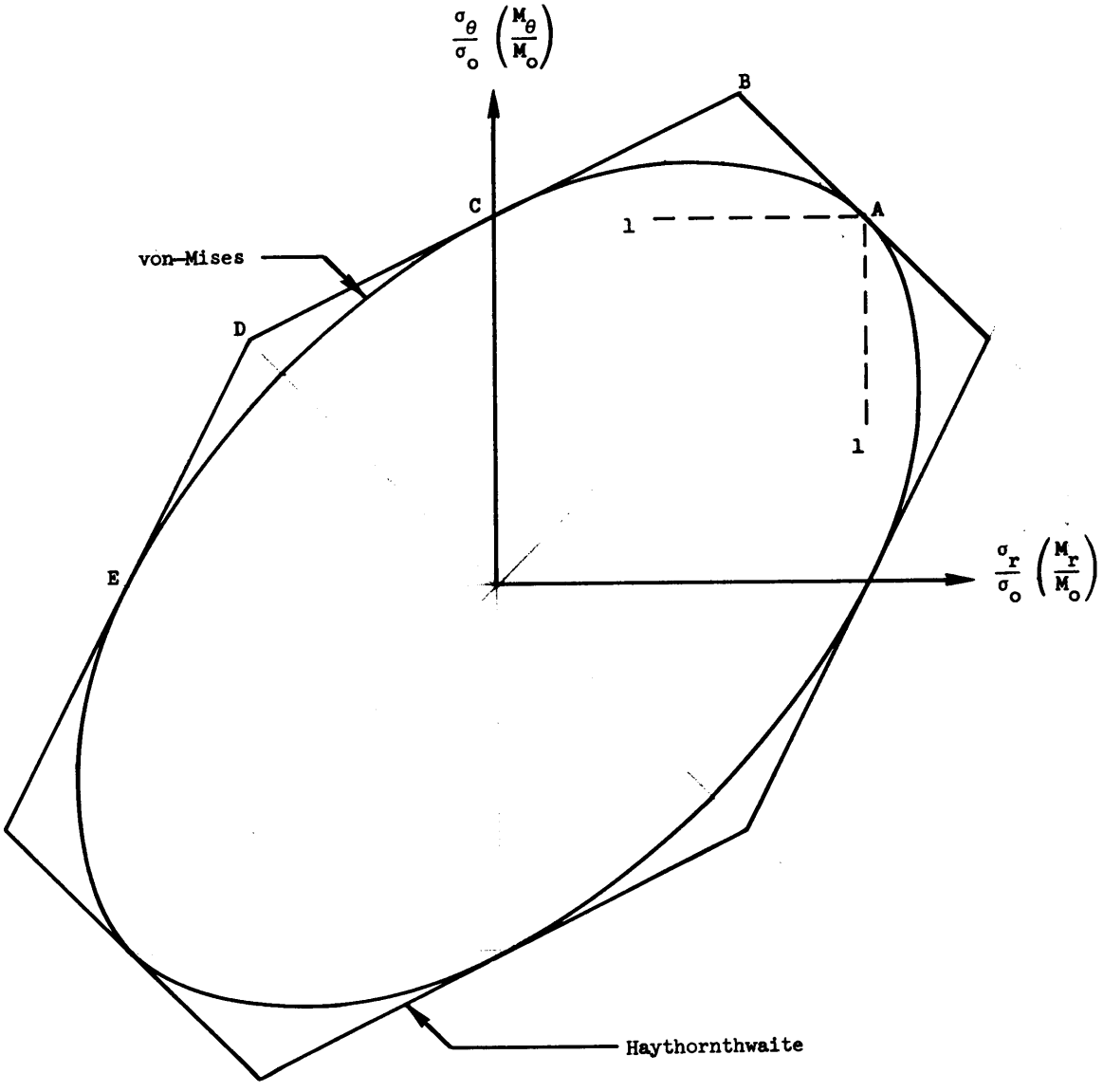

Figure 3. – Yield surfaces for von-Mises and Haythornthwaite yield conditions for plane stress problems.

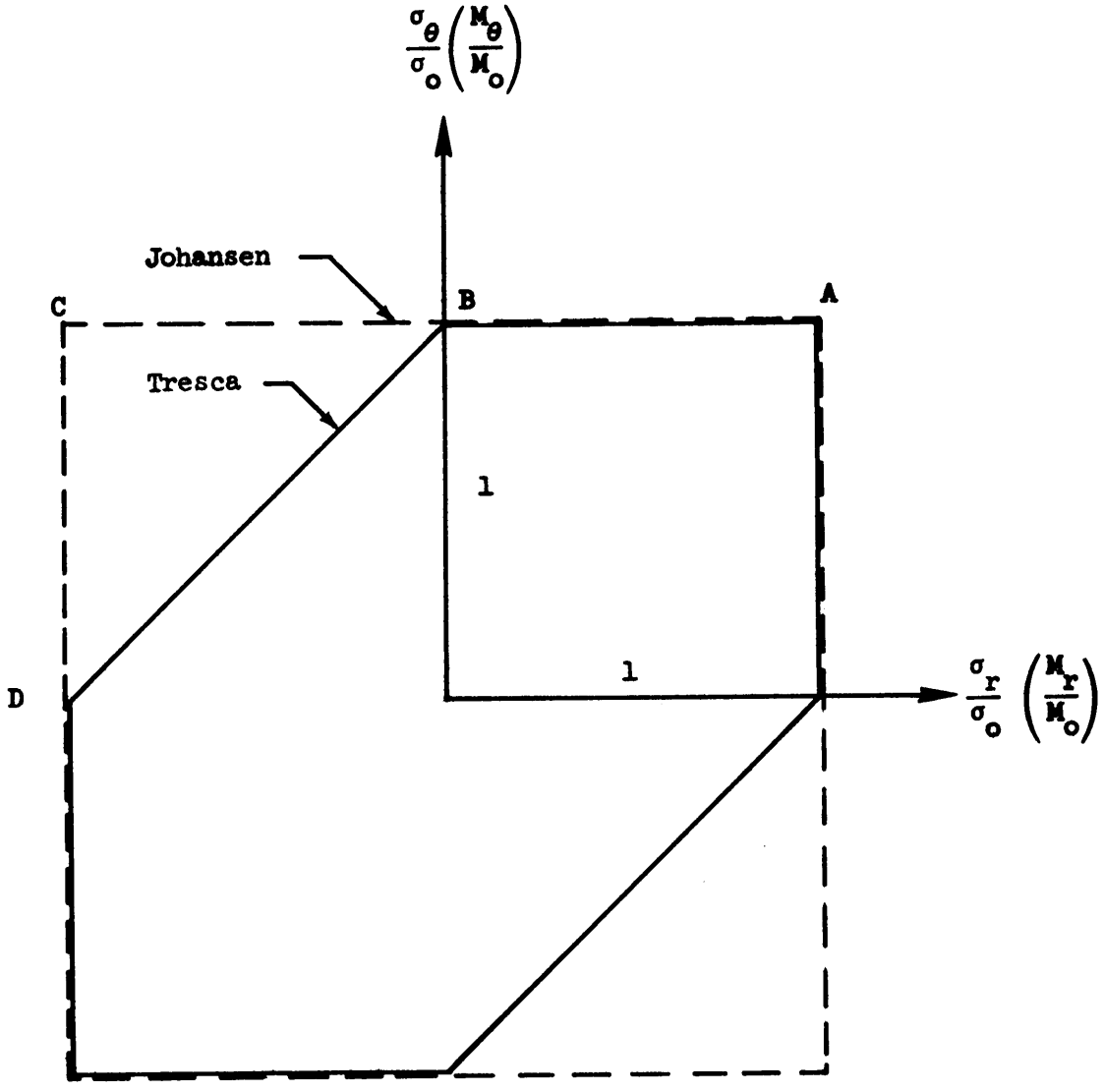

Figure 4. – Yield surfaces for Tresca and Johansen yield conditions for plane stress problems.

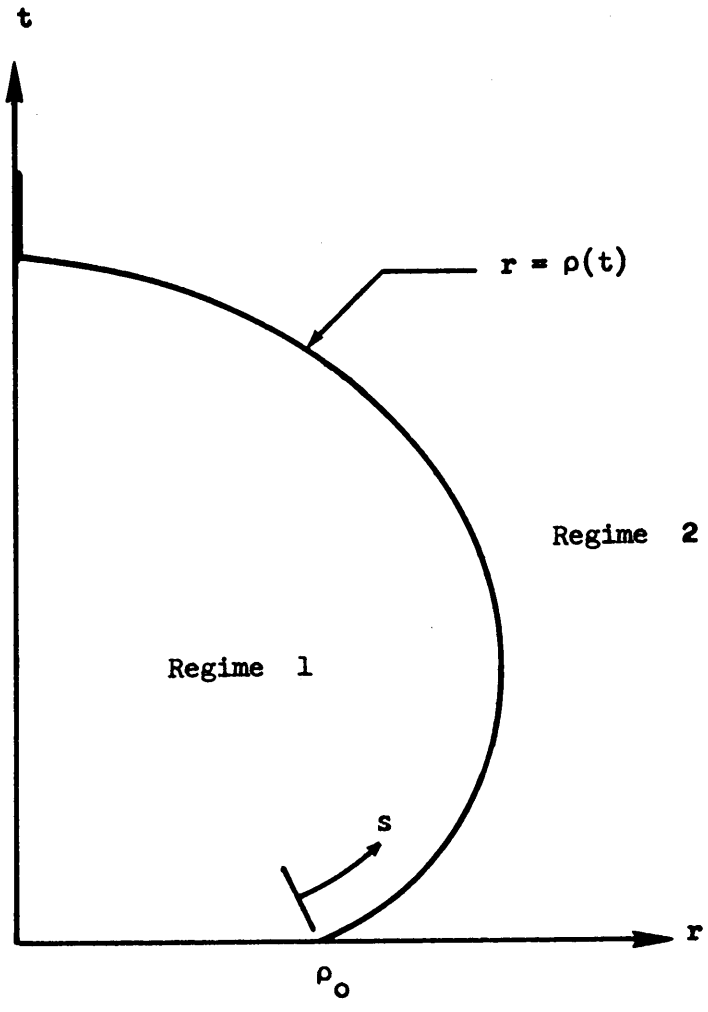

Figure 5. — General motion of a circle of discontinuty.

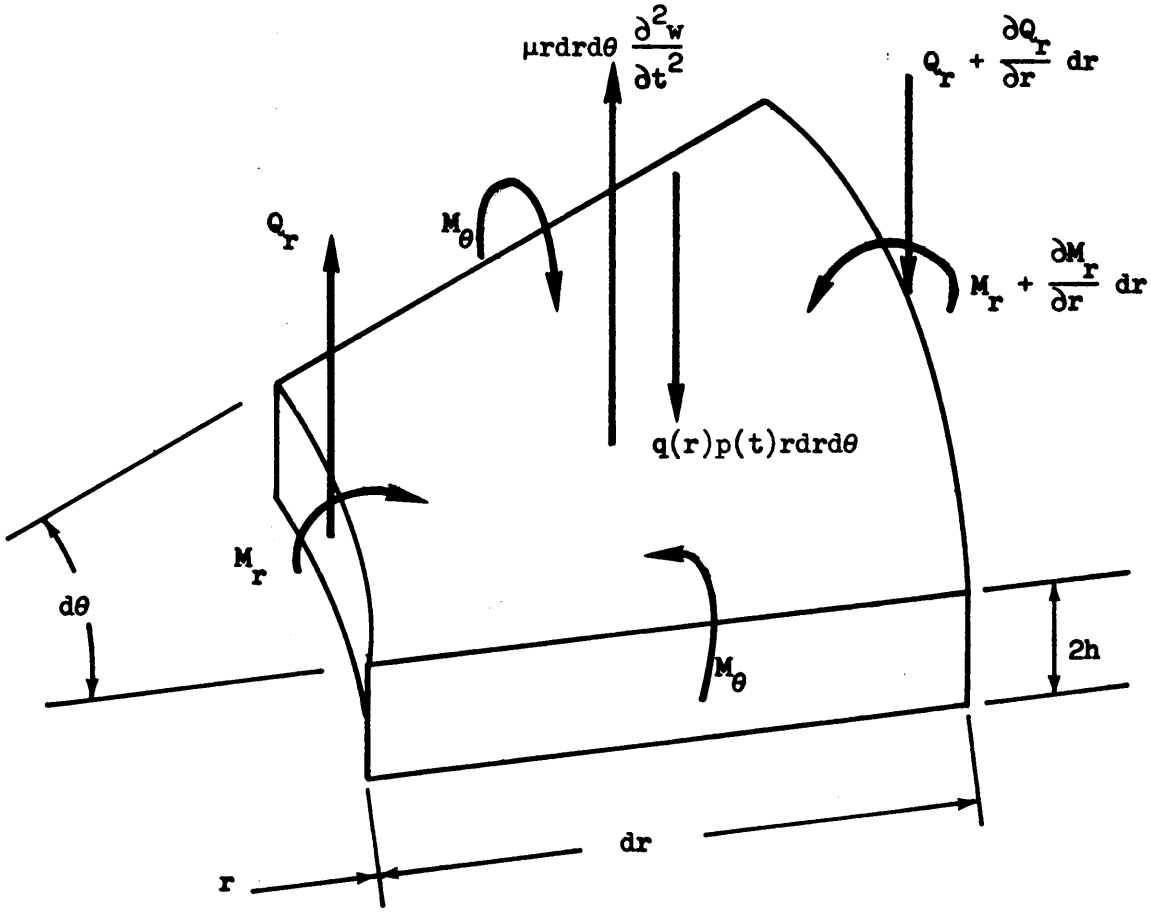

Figure 6. – Applied forces and moments on plate element.

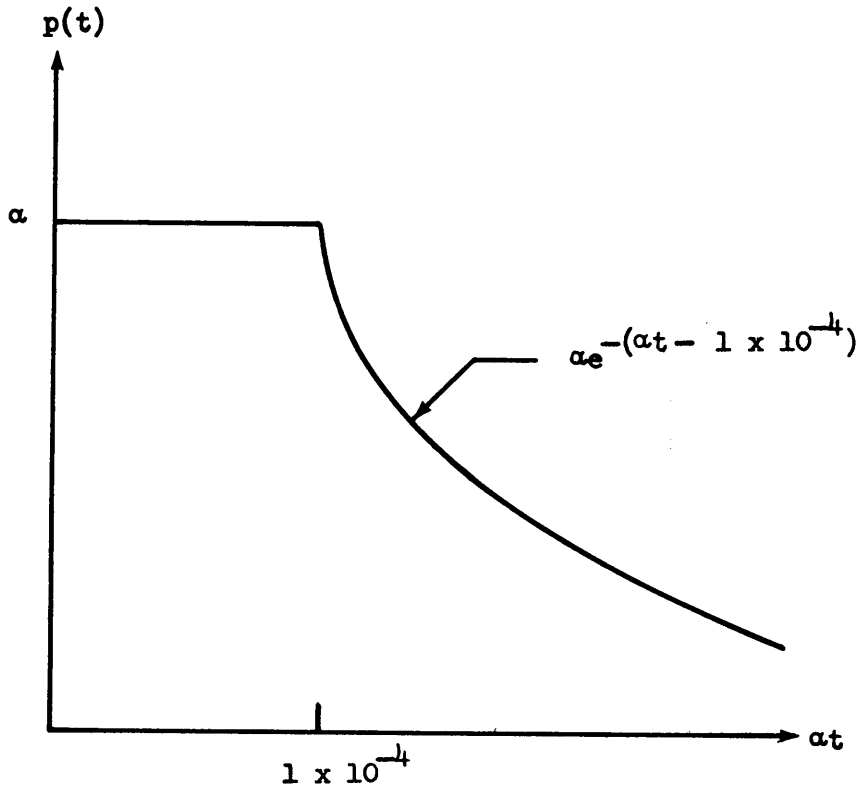

Figure 7. – General time variation allowed for example cases.

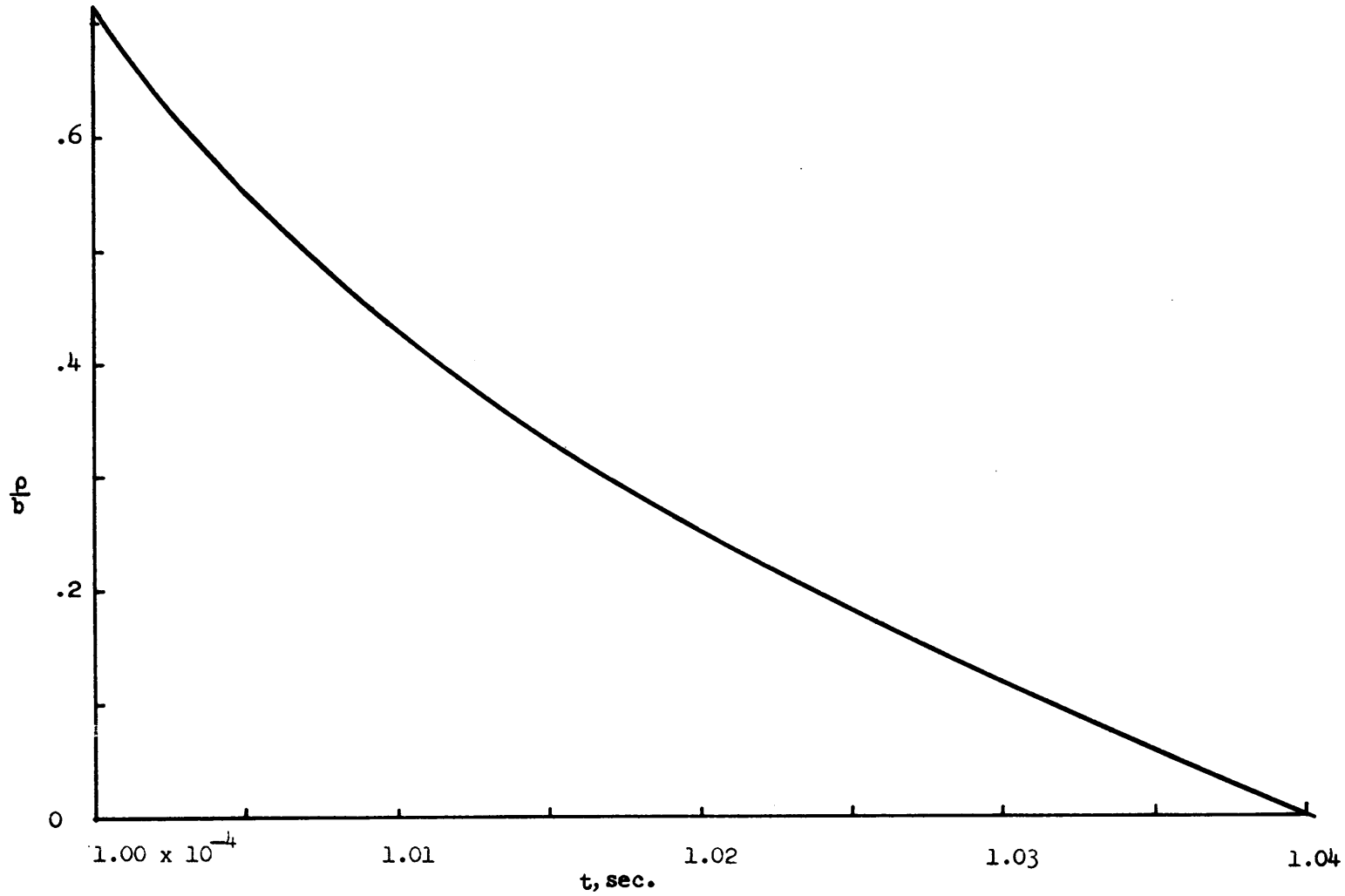

Figure 8. – Hinge circle movement for example case 1.

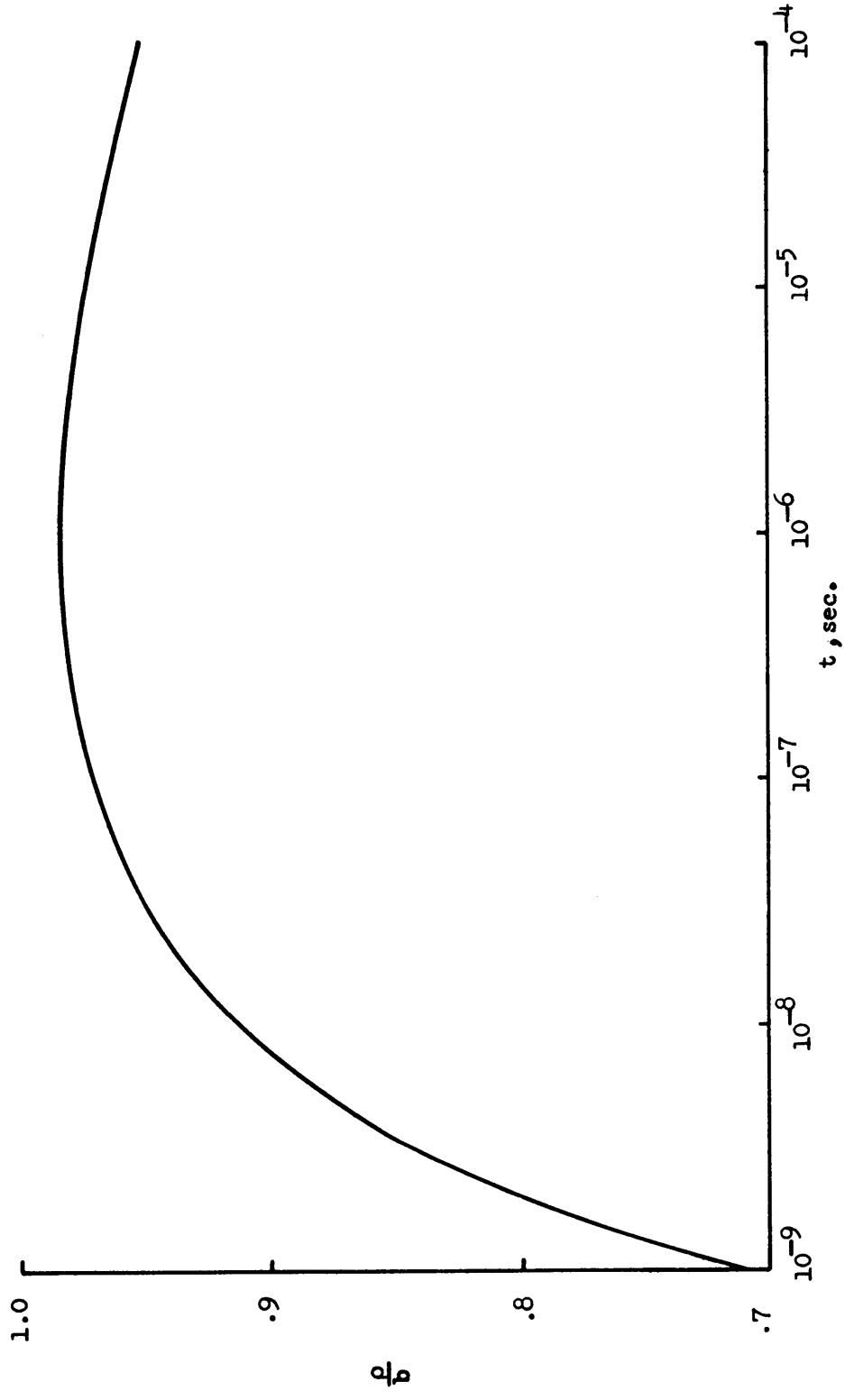

Figure 9. - Hinge circle movement for example case 2.

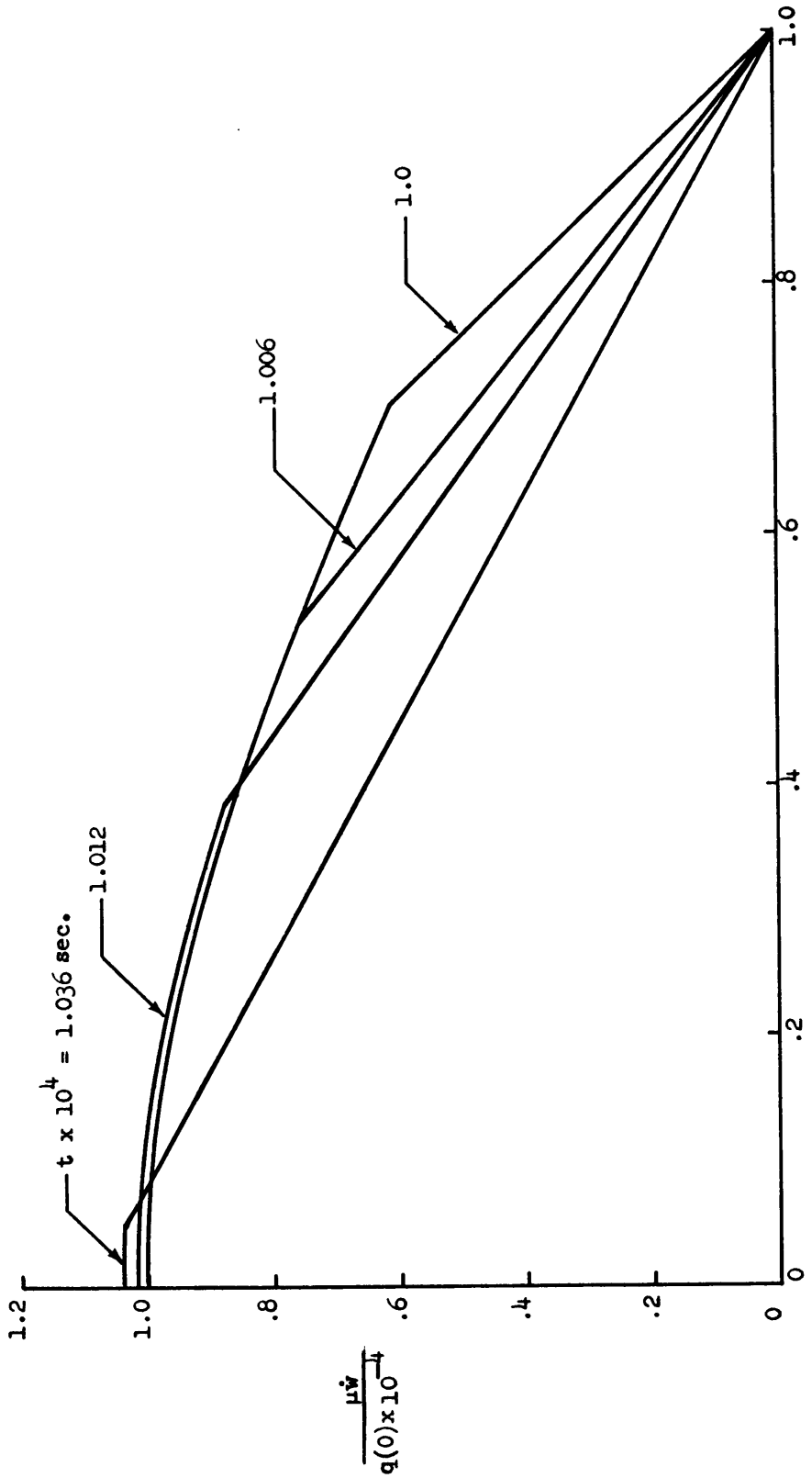

Figure 10. — Velocity distributions for various times for example case 1.

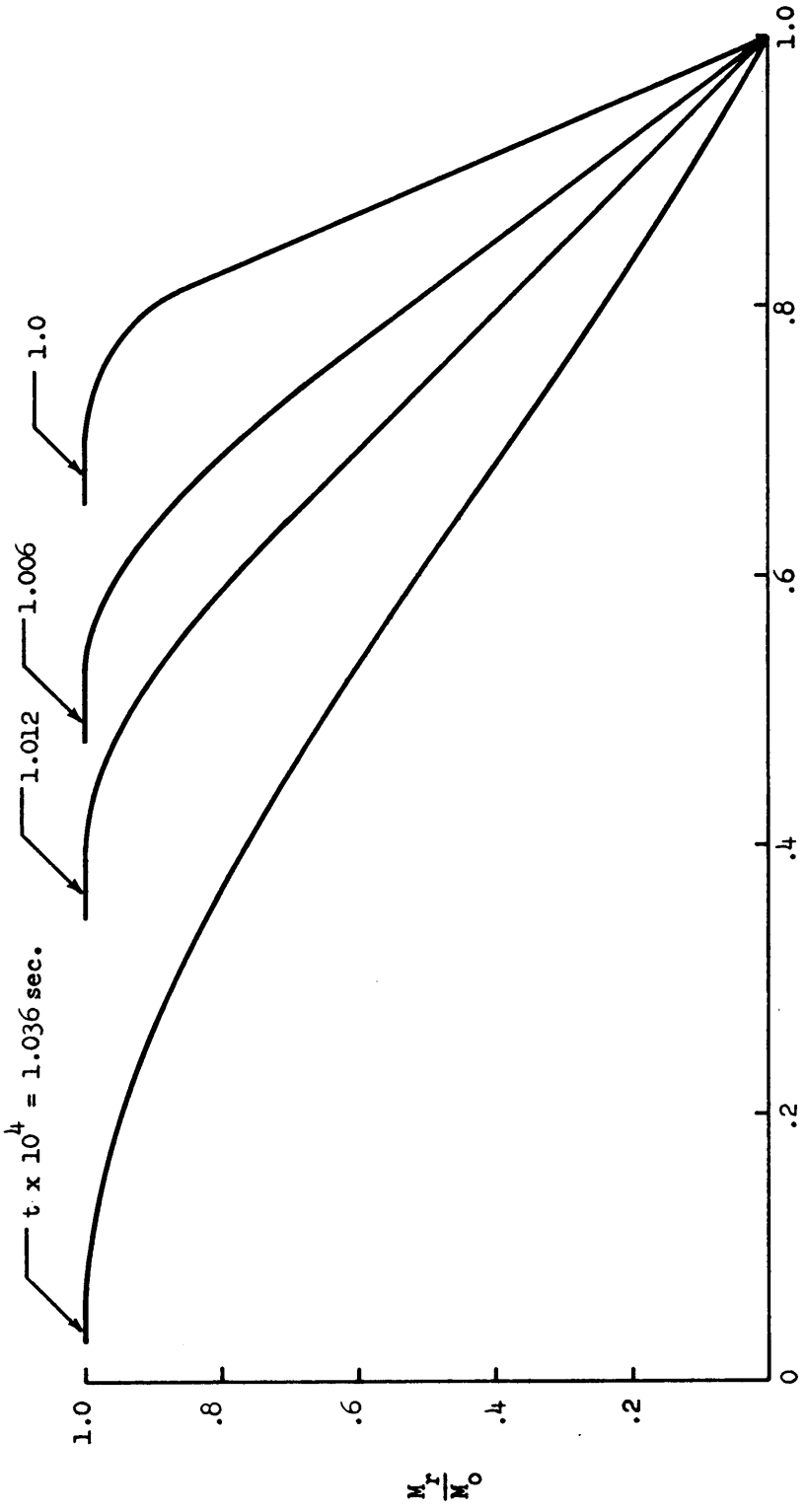

Figure 11. — Moment distributions for various times for example case 1.

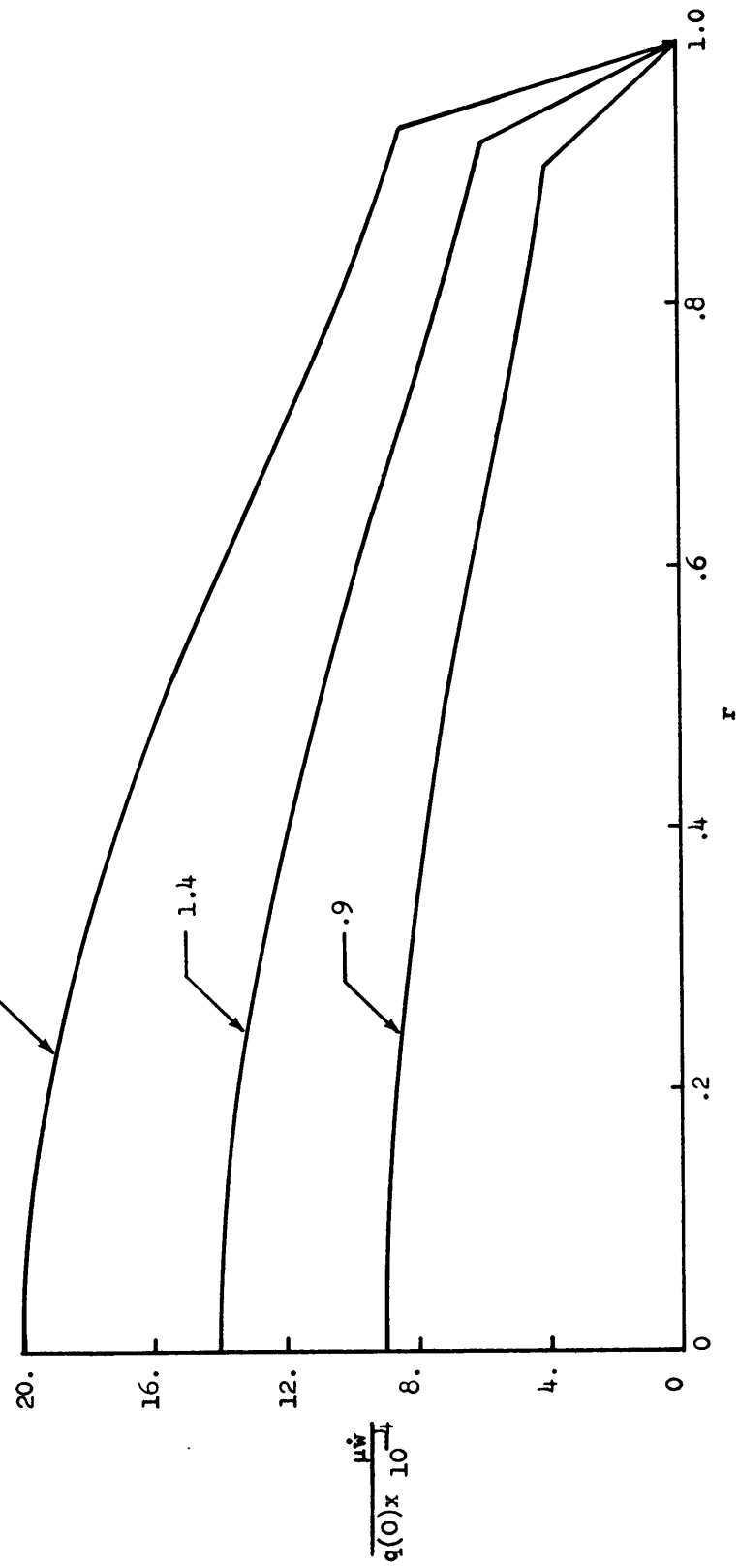

Figure 12. - Velocity distributions for various times for example case 2.

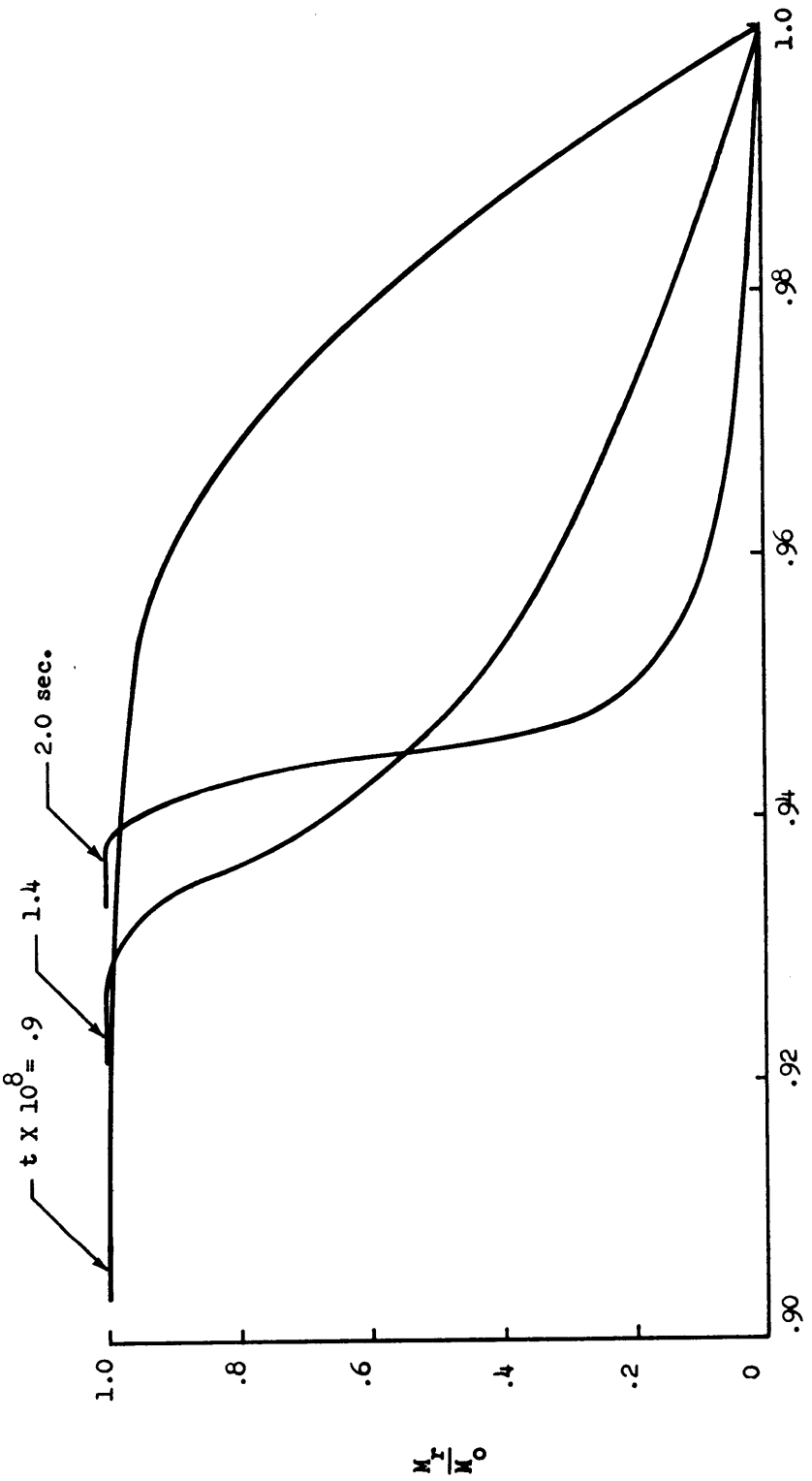

Figure 13. — Moment distributions for various times for example case 2.

RESPONSE OF A PLASTIC CIRCULAR PLATE TO A DISTRIBUTED TIME-VARYING LOADING

By

Deene J. Weidman

ABSTRACT

The bending response of a plate to dynamic loading has been of interest in plasticity theory for some time. Generally, many restrictive assumptions are made on both the material behavior and the loading applied to the plate. The plate material is considered rigid-plastic, and four basic yield criteria are discussed and evaluated, with the Tresca yield condition being selected from these four criteria as allowing the most generality of solution. This dissertation, however, removes the restrictions made concerning the applied loading for the Tresca yield condition. The plate is considered to be simply supported, and therefore, only one point (or circle) of discontinuity is considered to exist across the plate radius. The location of this circle of discontinuity is not generally constant but varies with time. The movement of this "hinge circle" is the key to solution of plastic plate problems under general loadings that vary with radius and time. The differential equation that defines the motion of the hinge circle is derived, and solved exactly for some cases. A short computer program is also presented that allows the numerical solution of the general non-linear differential equation for hinge circle location.

Many previous authors have considered the radial loading distribution to be either a partially (or fully) uniform radial distribution or

else a "concentrated" load, and either statically or impulsively applied in time. A few papers allowing slightly more general loadings are available, but in all previous work the authors make assumptions that require the radial location of the hinge circle to decrease with time. This assumption simplified the solution of the problem considerably, but it is not a valid assumption in general. In the present approach, the hinge circle is allowed to move as the loading dictates, and outward hinge motion is seen to occur. In some cases of general loading, the hinge circle does only move inward, but the actual rate of deflection could not have been calculated by previous analyses. Eventually, however, the hinge moves to the center of the plate, and the plate deforms conically until the hinge circle finally disappears, leaving a rigid, deformed plate. All of the quantities of interest (plate velocity, bending moments, stresses, etc.) are written in terms of the variable hinge circle location. The location of the hinge circle is then defined in the general case.